

5-2011

Computational study of Passive Neutron Albedo Reactivity (PNAR) measurement with fission chambers

Sandra De La Cruz
University of Nevada, Las Vegas

Follow this and additional works at: <https://digitalscholarship.unlv.edu/thesesdissertations>



Part of the [Materials Chemistry Commons](#), [Mechanical Engineering Commons](#), [Nuclear Engineering Commons](#), and the [Oil, Gas, and Energy Commons](#)

Repository Citation

De La Cruz, Sandra, "Computational study of Passive Neutron Albedo Reactivity (PNAR) measurement with fission chambers" (2011). *UNLV Theses, Dissertations, Professional Papers, and Capstones*. 1403. <https://digitalscholarship.unlv.edu/thesesdissertations/1403>

This Thesis is protected by copyright and/or related rights. It has been brought to you by Digital Scholarship@UNLV with permission from the rights-holder(s). You are free to use this Thesis in any way that is permitted by the copyright and related rights legislation that applies to your use. For other uses you need to obtain permission from the rights-holder(s) directly, unless additional rights are indicated by a Creative Commons license in the record and/or on the work itself.

This Thesis has been accepted for inclusion in UNLV Theses, Dissertations, Professional Papers, and Capstones by an authorized administrator of Digital Scholarship@UNLV. For more information, please contact digitalscholarship@unlv.edu.

COMPUTATIONAL STUDY OF PASSIVE NEUTRON ALBEDO REACTIVITY
(PNAR) MEASUREMENT WITH FISSION CHAMBERS

by

Sandra De La Cruz

Bachelor of Science
University of Nevada, Las Vegas
2008

A thesis submitted in partial fulfillment of
the requirements for the

Master of Science Degree in Materials and Nuclear Engineering
Department of Mechanical Engineering
Howard R Hughes College of Engineering

Graduate College
University of Nevada, Las Vegas
May 2011

Copyright by Sandra De La Cruz, 2011
All Rights Reserve



THE GRADUATE COLLEGE

We recommend the thesis prepared under our supervision by

Sandra De La Cruz

entitled

**Computational Study of passive Neutron Albedo Reactivity (PNAR)
Measurement with Fission Chambers**

be accepted in partial fulfillment of the requirements for the degree of

Master of Science in Materials and Nuclear Engineering

Department of Mechanical Engineering

William Culbreth, Committee Chair

Denis Beller, Committee Member

Robert Boehm, Committee Member

Gary Cerefice, Graduate Faculty Representative

Ronald Smith, Ph. D., Vice President for Research and Graduate Studies
and Dean of the Graduate College

May 2011

ABSTRACT

Computational Study of Passive Neutron Albedo Reactivity (PNAR) Measurement with Fission Chambers

by

Sandra De La Cruz

Dr. William Culbreth, Examination Committee Chair
Professor of Mechanical Engineering
University of Nevada, Las Vegas

The Passive Neutron Albedo Reactivity technique (PNAR) was used to assay used nuclear fuel as a potential method for the measurement of fissionable material in fuel assemblies. A Monte Carlo transport code (MCNPX 2.6) was used to develop simulation models to evaluate the PNAR technique. The MCNPX simulated models consisted of two 17x17 Pressurized Water Reactor (PWR) used fuel assemblies; one with an initial 3 wt% uranium-235¹, cooled for 20 years and second with an initial 4 wt% uranium-235², cooled for 5 years. Each used fuel assembly was simulated at four different burn up rates of 15, 30, 45, and 60 GWd/tU. Four fission chamber (FC) detectors were placed around the used fuel assembly. The four FC detectors considered in this study used Highly Enriched Uranium (HEU), Uranium Dioxide (UO₂), Depleted Uranium (DU) and Thorium (Th) FC detectors as the neutron detection material.

The purpose of this study as to understand the characteristics of PNAR method and to identify a FC detector system to analyze used nuclear fuel assemblies. Results showed HEU FC detectors responded better than the other FC detectors based on

¹ Referred as PWR Fuel Assembly 1

² Referred as PWR Fuel Assembly 2

cadmium ratio and on the precision counting time. The cadmium ratio response using the PNAR measurement technique with both PWR Fuel Assemblies 1 and 2, the HEU FC detector performed 0.3% better than UO₂, 3% better than DU and 30% better than thorium FC detectors. Based upon the detector counting time for both PWR fuel assemblies 1 and 2, the HEU FC detector's counting time was less than one minute, considerably less than the other three FC detectors.

ACKNOWLEDGEMENTS

I greatly appreciate the patience, support and guidance Dr. Denis Beller provided through this learning process, that it was above and beyond that can be given from a great professor. I would like to thank Dr. William Culbreth and Larry Lakeotes for their support and guidance.

TABLE OF CONTENTS

ABSTRACT	iii
ACKNOWLEDGEMENTS	v
LIST OF TABLES	viii
LIST OF FIGURES	ix
LIST OF ABBREVIATIONS	x
CHAPTER 1 INTRODUCTION	1
CHAPTER 2 REVIEW OF LITERATURE	3
Passive Neutron Albedo Reactivity (PNAR)	3
Nuclear Fuel Library	3
Cadmium Ratio	6
Previous Research	6
Fission Chamber Detectors	7
Detector Precision Limit	9
CHAPTER 3 METHODOLOGY	11
MCNPX	11
Geometry Model	11
Used Fuel Assembly	13
Fission Chambers	15
Neutron Fission Reaction Rate	16
Detector Counting Time Calculations	18
CHAPTER 4 RESULTS	20
Data Analysis	20
Cadmium Ratios	20
Detector Precision and Counting Times	26
Fissile Content Measurements	27
CHAPTER 5 CONCLUSIONS	33
APPENDIX I MCNPX INPUT	35
APPENDIX II OUTPUT	44
APPENDIX III CALCULATIONS	47
BIBLIOGRAPHY	48

VITA.....	50
-----------	----

LIST OF TABLES

Table I. MCNPX Used Fuel Assemblies Geometry Parameters. 14
Table II. Average Mass in PWR Fuel Assembly 1. 14
Table III. Average Mass in PWR Fuel Assembly 2. 15
Table IV. Fission Chamber Detector Parameters. 15
Table V. MCNPX Density for Fissile Material in FC detectors. 17
Table VI. MCNPX Data for Neutron Multiplication without Cadmium Layer. 21
Table VII. MCNPX Data for Neutron Multiplication with Cadmium Layer. 22
Table VIII. Cadmium Ratio Data for PWR Fuel Assembly 1..... 23
Table IX. Cadmium Ratio for PWR Fuel Assembly 2. 24
Table X. Minimum Counting Times for FC Detectors using PWR Fuel Assembly 1 at
45 GWd/tU. 26
Table XI. Minimum Counting Times for FC detectors using PWR Fuel Assembly 2 at 4
5 GWd/tU. 27
Table XII. Data for Cadmium Ratios with Pu-239 in PWR Fuel Assembly 1. 30
Table XIII. Data for Cadmium Ratios with Pu-239 in PWR Fuel Assembly 2. 30
Table XIV. Data for Cadmium Ratios with fissile mass in PWR Fuel Assembly 1. 31
Table XV. Data for Cadmium Ratios with fissile mass in PWR Fuel Assembly 2. 32

LIST OF FIGURES

Figure 1.	Mass Concentrations of Uranium-235 for PWR Fuel Assemblies 1 and 2 [2].	5
Figure 2.	Relative Plutonium Concentration for PWR Fuel Assembly 1 [2].	5
Figure 3.	XY-section of MCNPX geometry model.	12
Figure 4.	ZX-section of MCNPX geometry model.	13
Figure 5.	17x17 PWR used fuel assembly array	13
Figure 6.	Neutron multiplication without Cd layer for PWR Fuel Assemblies 1 and 2.	21
Figure 7.	Neutron multiplication with Cd layer for PWR Fuel Assembly 1 and 2.	22
Figure 8.	Cadmium Ratio for FC detectors using PWR Fuel Assembly 1.	23
Figure 9.	Cadmium ratio for FC detectors using PWR Fuel Assembly 2.	24
Figure 10.	PNAR response using the Cadmium Ratio for HEU and thorium FC.	25
Figure 11.	Cadmium Ratio with Pu-239 mass in PWR Fuel Assembly 1.	28
Figure 12.	Cadmium Ratio with fissile mass in PWR Fuel Assembly 1.	28
Figure 13.	Cadmium Ratio with Pu-239 mass in PWR Fuel Assembly 2.	29
Figure 14.	Cadmium Ratio with Fissile mass in PWR Fuel Assembly 2.	29
Figure 13.	Cadmium Ratio with Pu-239 in for HEU and Thorium FC Detectors.	30
Figure 14.	Cadmium Ratio with fissile mass in for HEU and Thorium FC Detectors	31

LIST OF ABBREVIATIONS

CR	Cadmium Ratio
DU	Depleted Uranium
FC	Fission Chamber
HEU	Highly Enriched Uranium
LANL	Los Alamos National Laboratory
MCNPX	Monte Carlo N-Particle eXtended
NDA	Non-Destructive Assay
NGSI	Next Generation Safeguards Initiative
PNAR	Passive Neutron Albedo Reactivity
PWR	Pressurized Water Reactor
SFM	Special Fissile Material
UO ₂	Uranium Dioxide
wt	weight

CHAPTER 1

INTRODUCTION

The safeguarding of nuclear material in used fuel assemblies has been thoroughly researched to reduce the risk of proliferation. The Next Generation Safeguards Initiative (NGSI) has identified the need for advanced instrumentation to measure the plutonium mass in used³ fuel assemblies [1]. The instrumentation developed can assist safeguards workers to account for the fissile material in used fuel assemblies during shipper and receiving or in reprocessing facilities. There are twelve candidate non-destructive assay (NDA) techniques that have been identified to have the capability to provide information about the composition of fissile material in used fuel assemblies [2]. These NDA techniques will need to be studied individually using a Monte Carlo transport code to evaluate their capability to assay used fuel assemblies.

The Passive Neutron Albedo Reactivity (PNAR) method is one of the twelve NDA techniques that will be evaluated. A Monte Carlo transport code (MCNPX 2.6) was used to develop simulation models to evaluate the PNAR technique. The MCNPX simulated models consisted of used fuel assemblies from a data library for Pressurized Water Reactors (PWR) created by Los Alamos National Laboratory (LANL) [3]. Four fission chamber (FC) detectors were placed around the used fuel assembly. MCNPX tallies were used to analyze the total neutron count in the FC detectors. A fission chamber is composed of three concentric cylinders containing aluminum, a thin layer of fissionable material (e.g. U-235) and gas. Highly Enriched Uranium (HEU) FC detectors have been previously used to evaluate the response of the PNAR technique [4]; however,

³ For this thesis used fuel and spent fuel are considered to be the same.

FC detectors contain a thin layer of fissionable material and they have not been evaluated with different fissionable material compositions. The PNAR technique was evaluated with four FC detectors using different fissionable material composition. The thin fissionable material layer in a FC detector was changed to compare their ability to assay used nuclear fuel.

The MCNPX simulated models used two 17x17 PWR used fuel assemblies; one with an initial 3 wt% U-235, cooled for 20 years and the other with an initial 4 wt% U-235, cooled for 5 years. Each used fuel assembly was simulated at four different burn up rates of 15, 30, 45, and 60 GWd/tU. The FC detector's thin layer of fissionable material was simulated using the following material compositions:

- 93 wt% ^{235}U and 7 wt% ^{238}U (HEU)
- 0.2 wt% ^{235}U , 99.8 wt% ^{238}U , and Oxygen (Depleted Uranium or DU)
- 19 wt% ^{235}U , 81 wt% ^{238}U , and Oxygen (Uranium Dioxide or UO_2)
- 100 wt% Thorium-232 (Thorium)

MCNPX was used as an aid to evaluate the PNAR measurement technique. The FC detectors were used to compare the PNAR response using two different used fuel assemblies at different burn up rates to determine the instrumentation system to use. The PNAR response was compared to the fissile mass and plutonium-239 in each of the used fuel assemblies to determine its capability to assay used nuclear fuel. In the following chapters, review of literature, methodology and results are discussed.

CHAPTER 2

REVIEW OF LITERATURE

Passive Neutron Albedo Reactivity (PNAR)

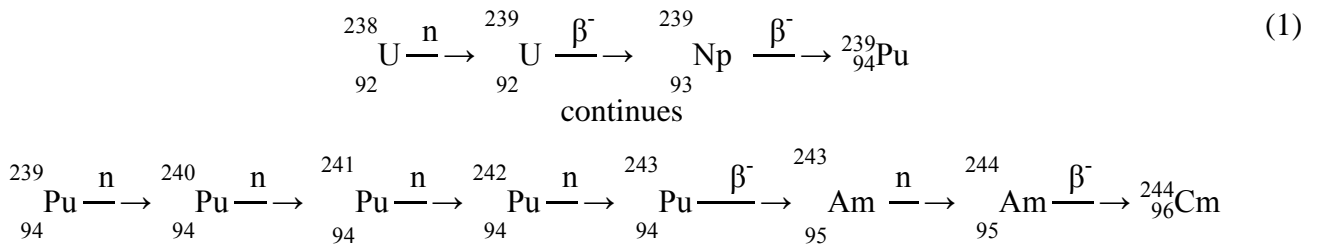
PNAR technique is based on the detection of naturally emitted neutrons from fissile material (such as U-235) in the used fuel assemblies. The neutrons result from the spontaneous fission of Cm-244 in the fuel assembly, which self-interrogates the fissile material [5]. This technique uses a 1 mm thick removable cadmium layer, located around the fuel assembly between the assembly and the FC detectors. The purpose of the cadmium layer is to obtain two measurements; one without the cadmium layer and one with it. The ratio of the total neutron count without the layer to total neutron count with the cadmium layer is known as the cadmium ratio. “The cadmium ratio scales with the fissile material in the used fuel assemblies [6].” With the cadmium layer in place slow neutrons with energy below 0.5 eV are absorbed, therefore changing the neutron energy spectrum that is reflected back into the fuel assembly. The addition of the cadmium layer decreases fission within the plutonium and uranium fissionable isotopes within the fuel assembly.

Nuclear Fuel Library

In support of NDA techniques research, Los Alamos National Laboratory created a library of simulated used fuel assemblies for Pressurized Water Reactors by estimating the amount of burn up predicted by MCNPX. The simulated used fuel assemblies had U-235 initial enrichments of 2, 3, 4, and 5%, cooling times of 1, 5, 20, and 80 years, and different total energy production levels (burn up) of 15, 30, 45 and 60 GWd/tU [6]. The purpose of the used fuel library is to provide the quantity of all isotopes in used fuel as a

function of burn up, initial enrichment and cooling time. In a PWR fuel assembly, the fuel pins are in a 17x17 array for a total of 264 pins. The simulated used fuel assemblies in the library contained different material composition for each pin, to represent the change in neutron flux that would exist within a fuel assembly while it was irradiated in a reactor.

As fuel in a reactor is used to produce energy, new isotopes are created as fission products, through radioactive decay, and through neutron activation. One of the isotopes created in used nuclear fuel is Cm-244 with a half-life of 18.11 years. The production of Cm-244 is important for the PNAR method, since it serves as the main source of spontaneous fission neutrons through its decay for the first 50 years that used fuel assemblies are left to cool out of the reactor core. Cm-244 spontaneous fission neutrons are used to self-interrogate the used fuel assemblies, since they can induce secondary fission within the U-235, Pu-239, and Pu-241 that remain in the used fuel. [7]. For example, in a 17x17 PWR fuel assembly with an initial 4 wt% U-235 enrichment, the following decay chain takes place:



As uranium isotopes are used for energy production in a reactor the mass of plutonium isotopes increase, including fissionable Pu-239 and Pu-241. Fissile Pu-239 decays to Cm-244. The following Figures 1 and 2 shown below are based on MCNPX data library for the two PWR used fuel assemblies from LANL showing that the mass of uranium decreases with burn up and plutonium isotopes mass concentrations increase [2].

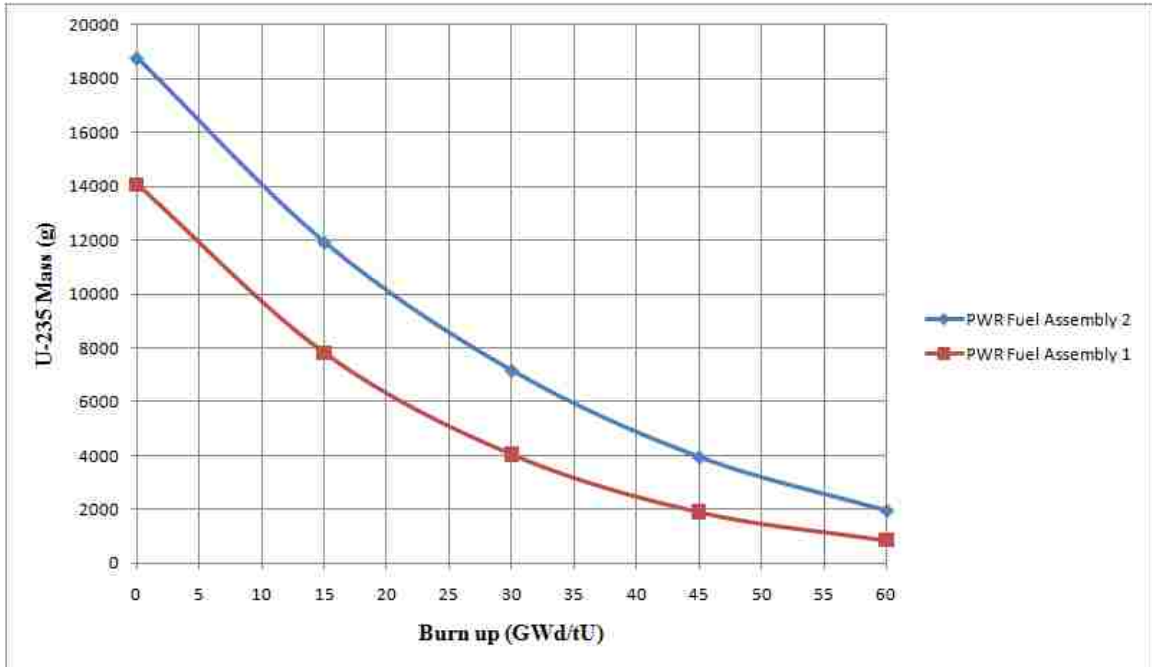


Figure 1. Mass Concentrations of Uranium-235 for PWR Fuel Assemblies 1⁴ and 2⁵ [2].

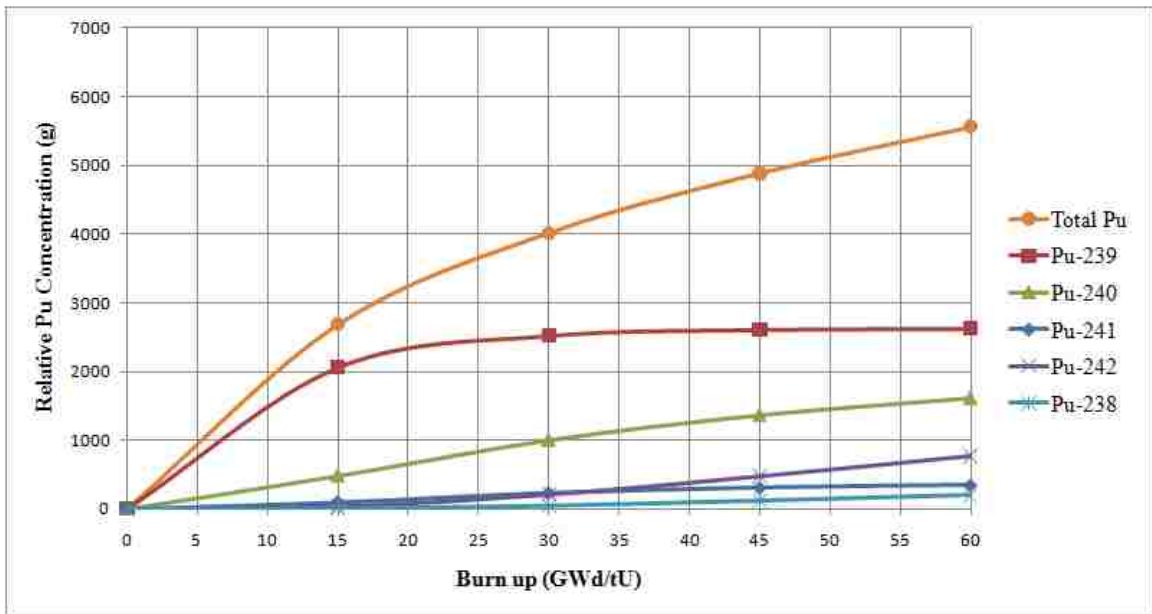


Figure 2. Relative Plutonium Concentration for PWR Fuel Assembly 1 [2].

The mass of uranium decreases as the fuel is used for energy production and the mass of plutonium increases through the absorption of fast neutrons within fertile U-238.

⁴ 3 wt% initial enrichment and cooled for 20 years

⁵ 4 wt% initial enrichment and cooled for 5 years

Cadmium Ratio

Cadmium has an absorption cross section of 2,450 barns for thermal neutrons, making it a useful neutron poison for the PNAR method. By comparison, boron has an absorption cross section of 759 barns, yet it is often used as a neutron poison to control criticality in a reactor coolant and in used fuel storage pools [8]. This technique uses a 1 mm thick removable cadmium layer, located around the fuel assembly between the assembly and the FC detectors to obtain the cadmium ratio. The cadmium ratio is based on two measurements; one without the cadmium layer and one with the cadmium layer. The cadmium layer was used to change the neutron spectrum that reaches the fission chamber detectors and the reflection of thermal neutrons back into the used fuel increases fission reactions; therefore, modifying the neutron flux spectrum. As previously discussed, the source of spontaneous fission neutrons within the used fuel is dominated by Cm-244. By surrounding the used fuel assemblies with the cadmium layer, most thermal neutrons below the energy of 0.5 eV are absorbed [9]. The absorption of neutrons below the cadmium cut-off energy of 0.5 eV, allows prompt neutrons from the spontaneous fission of Cm-244 to reach the FC detectors [2]. MCNPX tally results from simulations runs provided the data that was used to estimate the cadmium ratio.

Previous Research

MCNPX modeling of the PNAR method has been conducted at the Los Alamos National Laboratory using He-3 neutron detectors and HEU (93 wt% Uranium-235) FC detectors. Simulations of the PNAR combined with He-3 detector discovered that the fissile content in the used fuel assemblies changed with the cadmium ratio. Their model used 80 He-3 detectors which made it expensive to produce [6]. After, 9/11 there was a

He-3 shortage for use in neutron detectors and there is a high continuing demand making it expensive to acquire [10].

Through MCNPX modeling of the PNAR, it was found to be less expensive to build using four fission chambers. The fission chamber used contained 93% enriched uranium (HEU). The efficiency of fission chambers is lower than He-3 detectors; however, by comparing measurement times, the efficiency of the fission chambers is shown to be acceptable [4].

The PNAR technique was also analyzed using boron liquid scintillators. The PNAR technique was used to quantify the weighted sum of U-235, Pu-239 and Pu-241; however, it could not distinguish the contribution to the cadmium ratio resulting from each isotope. Boron liquid scintillators were found to perform better using a different NDA method known as the Differential Die-Away Self-Interrogation (DDSI) compared to using the PNAR method due to the scintillators die-away characteristics [2].

Fission Chamber Detectors

Fission chamber (FC) detectors are neutron detectors that use a thin coating of electroplated fissile material to generate highly ionized fission fragments through nuclear fission that are subsequently counted in a proportional chamber. The electroplated coating typically consists of a fissionable material, such as highly enriched uranium that is more than 90 wt% U-235 [11]. The most common FC detector used is highly enriched at 93 wt % U-235[12]. A fission chamber is composed of concentric cylinders with an outer aluminum layer, a fissile material coating and gas. The most common gas used is 97% argon mixed with 3% nitrogen.

For this study, FC detectors with and without gas were compared. The interactions of interest are not in the ionization or activation range in the gas. In comparing the MCNPX modeling of He-3 detectors and FC detectors, He-3 detectors rely upon the impact of neutrons on He-3 resulting in the production of tritium and a proton. Both of these charged particles are easily measured in a proportional detector. FC detectors depend upon the neutron interactions with the fissile material coating within the proportional counter tube. For FC detectors, MCNPX tallies will be used to monitor the neutron absorption within the fissile coating of the detector to infer the production of ionized fission products that can be readily measured by the proportional counter.

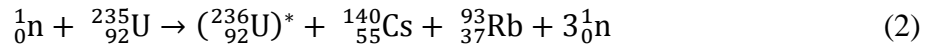
Another difference between FC detectors and He-3 detectors is that lead is not needed to shield gamma radiation. FC detectors are sensitive to thermal neutrons, but not to gamma radiation exposure [12]. The four FC detectors used in this study included:

- 93 wt% ^{235}U and 7 wt% ^{238}U (HEU)
- 0.2 wt% ^{235}U , 99.8 wt% ^{238}U , and Oxygen (Depleted Uranium or DU)
- 19 wt% ^{235}U , 81 wt% ^{238}U , and Oxygen (Uranium Dioxide or UO_2)
- 100 wt% Thorium-232 (Thorium)

U-235 Fission Chamber Detectors

FC detectors depend on neutron interactions with the fissile material coating. HEU, UO_2 , and DU FC detectors contain fissionable material U-235. U-235 is a fissile material that has a high probability to fission with thermal neutrons. The thermal neutron fission cross-section is 580 barns [11]. When a neutron interacts with fissile uranium, an excited U-236 isotope is created. This unstable isotope fission releasing large amounts of energy totaling about 200 MeV. During the fission process, the unstable isotope splits

into two large fission fragments and releases about three neutrons. These prompt fission neutrons were tallied in the FC detectors using MCNPX. The neutron and uranium reaction is shown below:



The other isotopes present in the thin fissile coating include U-238 and oxygen which do not fission with thermal neutrons. U-238 is a fertile isotope meaning that it can transmute into fissionable Pu-239. Oxygen has a relatively low absorption cross-section about 3.76 barns for thermal neutrons and does not greatly affect the results.

Thorium-232 Fission Chamber Detectors

Thorium-232 is a fertile isotope which is relatively inexpensive, so it was considered as a possible FC coating material. Fertile isotopes tend to absorb fast neutrons with energies above 1 eV and ultimately decay to fissile materials [8]. Fast neutron absorption in Th-232 results in the production of fissionable U-233. The thorium FC detector modeled in this study will not tend to react with any thermal neutrons, only with fast neutrons emitted from the used fuel assemblies.

Detector Precision Limit

The detector precision limit was used to compare the MCNPX FC detector model results to real-world detectors. MCNPX, a Monte Carlo simulation code, provides a statistical uncertainty in any measurement based on the total number of counts obtained in a tally. For the four FC fissile coatings studied in this work, the Detector Precision Limit is defined as the amount of counting time that a detector would have to operate to produce the same statistical uncertainty.

The MCNPX uncertainty was given in the computer readout for each tally. In order to compare the performance of each of the four candidate fissile coatings, the counting time for an actual detector was estimated based on the number of fissions produced in the coating per incident thermal neutron. The incident thermal neutrons were produced from the sample fuel assemblies. The counting time was adjusted for each coating material to produce the same statistical uncertainty as reported by MCNPX. Sampling efficiency, to be useful, needs to be within a 1-sigma precision of 0.5% to 1.0% for each tally [13]. This detector precision limit was used to determine the counting time in a real detector system. LANL conducted 28 hours of counting statistics using the Epithermal Neutron Multiplicity Counter (ENMC), to determine the electronics precision limit to be 0.05% for a single measurement [14]. If the real-world precision or relative uncertainty is set to 0.05%, then the number of counts necessary for that precision can be determined.

$$\text{relative uncertainty} \pm \frac{1}{\sqrt{N}}, \text{ where } N \text{ is the number of counts} \quad (3)$$

Solving for the number of counts to attain a 0.05% uncertainty, the total required number of counts is 4×10^6 . The MCNPX tally results were used to calculate the count rate of neutrons in the FC detectors and to estimate the uncertainty [4]. The counting times need to be less than 60 seconds, in order to process as many used fuel assemblies as possible. Large counting times will not be useful, because it will be time consuming and the Detector Precision Limit provides a useful comparison of the four candidate fissile coating materials. For each candidate fissile coating, we can determine if they will provide enough counts within 60 seconds to yield a 0.05% uncertainty in the measurement.

CHAPTER 3
METHODOLOGY

MCNPX

The Monte Carlo N-Particle eXtended transport code (MCNPX) version 2.6 was used to create model simulations to analyze the PNAR measurement technique using different material composition for the thin coating of fissionable material in FC detectors. MCNPX is a code used for the transport and generation of particles, such as neutrons [15]. The fission cross-sections of fissile material have been bench marked with previous experiments containing fissile material conducted in 1968 and 1969. The findings showed MCNPX results agreed with the experimental measurements conducted, confirming the accuracy of MCNPX models using fission cross-sections [16].

The PNAR technique interrogates the used fuel by analyzing the cadmium ratio, which is the ratio between two neutron count rate measurements with and without the Cd layer. The two measurements differ in the neutron energy spectrum reflected back into the used fuel. The cadmium ratio is considered to “scale with fissile content” in used nuclear fuel [1]. MCNPX was used to tally the prompt neutrons in the thin layer of fissionable material in the FC detectors. A multiplication card in MCNPX allows the user to conduct additional calculations. The multiplication card was used to calculate total fission neutrons in the FC detector’s thin material coating. MCNPX results were used to calculate the cadmium ratio and the counting times.

Geometry Model

The MCNPX simulation model contained a 17x17 PWR used fuel assembly in the center surrounded by borated water. Four FC detectors were placed around the used fuel

assembly embedded in 5 cm of polyethylene. Polyethylene was used to scatter fast neutrons or slow them down to lower energies, in order to increase the neutron fissions within the coating of fissionable material. The FC detector was placed parallel to each side of the used fuel assembly to maximize the incident area.

A 1 mm thick removable cadmium layer was placed around the fuel assembly between the assembly and the FC detectors; therefore, two geometries were required to implement the PNAR technique. The first geometry was modeled with the cadmium layer and the other one without cadmium layer.

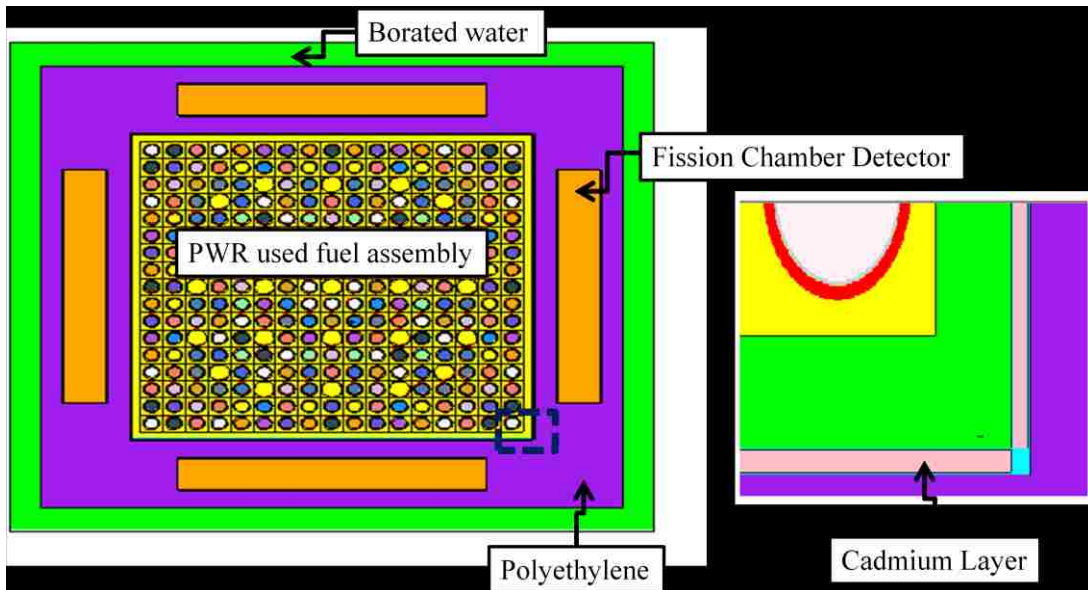


Figure 3. XY-section of MCNPX geometry model.

The different colors represent the material composition: the purple represents the polyethylene, green is borated water, and yellow denotes the fission chamber detectors. The small cut out of the XY-section, shows the location of the cadmium layer.

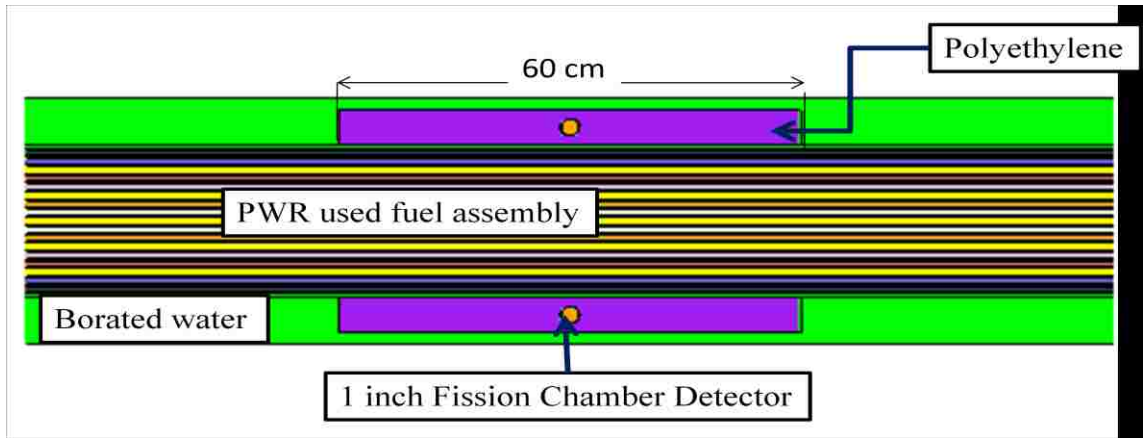


Figure 4. ZX-section of MCNPX geometry model.

Used Fuel Assembly

Two 17x17 PWR used fuel assemblies were simulated in MCNPX from the nuclear used fuel library. The first used fuel assembly modeled was with an initial 3 wt% U235 enrichment and was cooled for 20 years. The second used fuel assembly was with an initial 4 wt% U-235 enrichment and was cooled for 5 years. Both fuels were used at energy production levels of 15, 30, 45, and 60 GWd/tU. A cross-section of the 17x17 PWR used fuel assembly array is shown in Figure 5. It illustrates the locations of fuel pins, instrument tube, and control rod guide tubes.

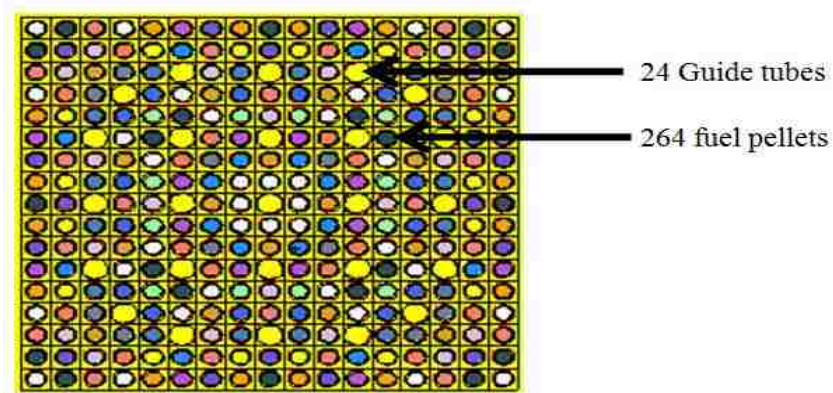


Figure 5. 17x17 PWR used fuel assembly array

The simulated fuel pins contain different material cards to represent the burn-up rate depending on the location of the assembly in a reactor.

Table I. MCNPX Used Fuel Assemblies Geometry Parameters.

Parameter	Description
Used Fuel Composition	3 wt%, 20 year cooled at 15, 30, 45, 60 GWd/tU
	4 wt%, 5 year cooled at 15, 30, 45, 60 GWd/tU
Active fuel height	365.76 cm
Pellet diameter	0.820 cm
Fuel pins in assembly	264
Assembly array	17 x 17
Pin pitch	1.26 cm
Clad thickness	0.065 cm
Clad material	Zircaloy-2/ M-5 (5.8736 g/cc)
Guide tubes	24
Instrument tube	1
Inner radius	0.571 cm
Outer radius	0.613 cm

Each of the PWR fuel assemblies modeled weighs about 533 kilograms. About 80% of the mass in used fuel assemblies is U-238. U-238 is a fertile isotope meaning that it can transmute into fissionable Pu-239, as the mass of U-238 decreases Pu-239 mass increases. The average mass in an assembly for the fissile materials of interest, U-235, Pu-239, Pu-241, and Cm-244 either increased or decreased with burn up. Tables II and III illustrated the mass concentrations for PWR Fuel Assemblies 1 and 2.

Table II. Average Mass in PWR Fuel Assembly 1.

Burn up (GWd/tU)	U-235 (grams)	Pu-239 (grams)	Pu-241 (grams)	Cm-244 (grams)
15	7813	2062	95	0.23
30	4051	2524	230	6.5
45	1908	2610	307	34
60	858	2624	345	93

Table III. Average Mass in PWR Fuel Assembly 2.

Burn up (GWd/tU)	U-235 (grams)	Pu-239 (grams)	Pu-241 (grams)	Cm-244 (grams)
15	11916	2070	157	0.19
30	7150	2686	438	6.1
45	3936	2779	632	37
60	1946	2817	724	112

The individual modeling for each fuel pin will make it easier to change the fuel composition, if needed for future MCNPX simulations.

Fission Chambers

The FC detectors in MCNPX were modeled as concentric cylinders with aluminum, fissile material and gas content of 97% argon mixed with 3% nitrogen. The thickness of the fissile material was modeled using 3 mg/cm² of fissile material, equivalent to a thickness of about 1.6x10⁻⁴ cm. Table III shows the FC detector parameters, the thin layer of fissionable material was the only modification in the simulated FC detector geometry.

Table IV. Fission Chamber Detector Parameters.

Parameter	Description
Length	17 cm (~7 inches)
Diameter	1 inch
Fissile material layer	thickness-1.6x10 ⁻⁴ cm 3 mg/cm ² of fissile material
Isotopic Composition	
FC Detector 1(HEU)	U-235 93 wt.% 7% U-238 19% U-235
FC Detector 2 (UO ₂)	81% U-238 Oxygen 0.2% U-235
FC Detector 3 (DU)	99.8% U-238 Oxygen
FC Detector 4 (Th)	100% Th-232

The FC detectors were placed as close as possible around the used fuel assembly. The location of FC detectors is significant because through a distance of 10 cm the neutron signal decreased by a factor of 10 [17].

Neutron Fission Reaction Rate

The tally multiplication card in MCNPX was used to obtain the fission reaction rate in the thin layer of fissionable material from the flux tally for each FC detector. MCNPX tally results provided the neutron flux in units of neutrons/cm² per source neutron. The multiplication card was used to obtain the neutron-to-fission reaction (n, f) by placing a “-6” in the MCNPX input. The multiplication card was used in the following manner for each FC detector:

F14: n (cell number for fissionable material in FC detector)

Fm14 -1 316 -6

Sd14 1

The multiplication card (Fm) directs MCNPX using “-1” to multiply the flux tally (neutrons/cm² per source particle) by the atom density of material “316”, which in this case belongs to HEU FC detector. The flux tally was also multiplied by the microscopic neutron-to-fission reaction cross section in barns for material “316” [15]. The Sd card multiplied the tally by volume for the specified cell number. The final tally results are needed in units of count per source neutron, to calculate the counting time.

For example using HEU FC detector, the following calculations were completed:

$$\begin{aligned} \text{Volume} &= \pi * \text{radius}^2 * \text{height} & (4) \\ &= \pi * \left(1.6 \times 10^{-4} \text{ cm}\right)^2 * 17 \text{ cm} \\ &= 2.15 \times 10^{-2} \text{ cm}^3 \end{aligned}$$

The atom density for the thin fissionable material layer in HEU FC detector was calculated using equation 5, given 235.25 g/mole as the mass of HEU FC detectors thin layer (See Appendix III Calculation 1)

$$N(\text{atom density}) = \frac{18.95 \frac{\text{g}}{\text{cm}^3} * 6.02 \times 10^{23} \frac{\text{atoms}}{\text{mole}}}{235.252 \frac{\text{g}}{\text{mole}}} = 4.851 \times 10^{23} \frac{\text{atoms}}{\text{cm}^3} \quad (5)$$

or in atoms per barn-cm, it was converted using the following:

$$N = 4.851 \times 10^{23} \frac{\text{atoms}}{\text{cm}^3} * 1 \times 10^{-24} \frac{\text{cm}^2}{\text{barn}} \rightarrow N = 4.851 \times 10^{-2} \frac{\text{atoms}}{\text{barn-cm}}$$

Using the volume and atom density calculated above, the tally multiplier calculates the counts per source neutron in the thin fission material layer (See Appendix III Calculation 2). The densities used in MCNPX for the FC detectors are shown in Table V.

Table V. MCNPX Density for Fissile Material in FC detectors.

FC detector	Density (g/cm ³)
HEU	18.95
UO ₂	10.9
DU	18.95
Thorium	11.74

Detector Counting Time Calculations

The precision limit was used to calculate the counting time for each FC detector to compare the experimental MCNPX results to real-world detectors [4]. The real-world precision or relative uncertainty was set to 0.05%, and then the number of counts necessary for that precision can be determined.

$$\text{Time (Seconds)} = \frac{N \text{ (counts)}}{\text{count rate}} \quad (6)$$

where N represents the total counts to achieve a real-world precision of 0.05%, which is equivalent to 4×10^6 counts.

In order to estimate the neutron count rate detected by the FC detectors, the MCNPX results given by the multiplication card were multiplied by the spontaneous fission activity in the used fuel assembly per gram of Cm-244. The spontaneous fission neutron yield for Cm-244 is about 1.08×10^7 neutrons per second for each gram of Cm-244. For example, PWR Fuel Assembly 2 at 45 GWd/tU has about 36 grams of Cm-244, equating to a neutron emission rate of 3.92×10^8 n/s. This rate was multiplied by the MCNPX tally results for HEU FC detector to estimate the detected count rate.

$$\begin{aligned} \text{Count rate} &= 6.77 \times 10^{-4} \frac{\text{counts}}{\text{source neutron}} * 3.92 \times 10^8 \frac{\text{neutrons}}{\text{second}} \quad (7) \\ &= 2.65 \times 10^5 \frac{\text{counts}}{\text{second}} \end{aligned}$$

Using the count rate and spontaneous neutron emission rate, the acquisition time for the electronics precision limit was calculated as follows:

$$\text{Time} = \frac{4 \times 10^6 \text{ counts}}{2.65 \times 10^5 \text{ counts/seconds}} = 15 \text{ seconds} \quad (8)$$

The cadmium ratio and the counting times for each FC detector were analyzed and compared to evaluate the PNAR response.

CHAPTER 4

RESULTS

Data Analysis

MCNPX tallies were used to track the total neutron count in the thin fissile material layer of each FC detector. The results were used to calculate the cadmium ratio and the counting times. The cadmium ratio was used to measure the response of the PNR technique as the fuel was used for energy production. The counting times using a 0.05% precision was used to compare the MCNPX experimental results with real-world detector systems.

Cadmium Ratios

The cadmium ratio was calculated as the total neutron count without Cd layer to the total neutron count with Cd layer in place. The error propagation for the MCNPX tally uncertainties were calculated using the following equation:

$$\sigma_{\text{Cd Ratio}} = \sqrt{\sigma_{\text{woCd}}^2 + \sigma_{\text{wCd}}^2} \quad (9)$$

where, σ_{woCd} = MCNPX tally uncertainty without Cd

σ_{wCd} = MCNPX tally uncertainty with Cd

For simplicity, PWR used fuel assembly with initial 3 wt% U-235 and cooled for 20 years is referred as PWR Fuel Assembly 1. The PWR used fuel assembly with initial 4 wt% U-235 and cooled for 5 years is denoted as PWR Fuel Assembly 2.

The neutron multiplication within a fuel assembly affects the cadmium ratio. Without the cadmium layer, the neutron multiplication was higher compared to inserting the cadmium layer, due to more neutrons reflecting back in the fuel increasing neutron-to-fission

reactions. As fresh fuel was used for energy production, the neutron multiplication factor decreased as shown in the Figures 6 and 7 for both PWR fuel assemblies.

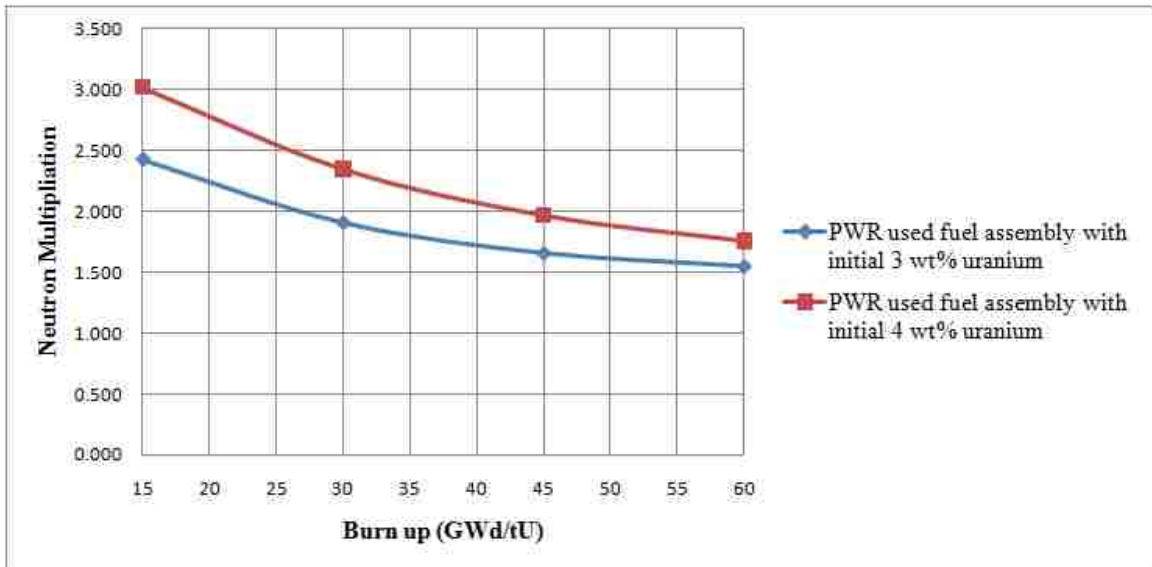


Figure 6. Neutron multiplication without Cd layer for PWR Fuel Assemblies 1 and 2. The neutron multiplication in PWR Fuel assembly 2 was higher due to the additional 1 wt% U-235 fissile mass.

Table VI. MCNPX Data for Neutron Multiplication without Cadmium Layer.

GWd/tU	PWR Fuel Assembly 1	PWR Fuel Assembly 2
15	2.429 ± 0.002	3.019 ± 0.003
30	1.908 ± 0.002	2.350 ± 0.002
45	1.656 ± 0.002	1.969 ± 0.002
60	1.547 ± 0.002	1.759 ± 0.002

Inserting the cadmium layer around the fuel assembly, the neutron multiplication decreased about 13% for PWR Fuel Assembly 1 and 17% for PWR Fuel Assembly 2.

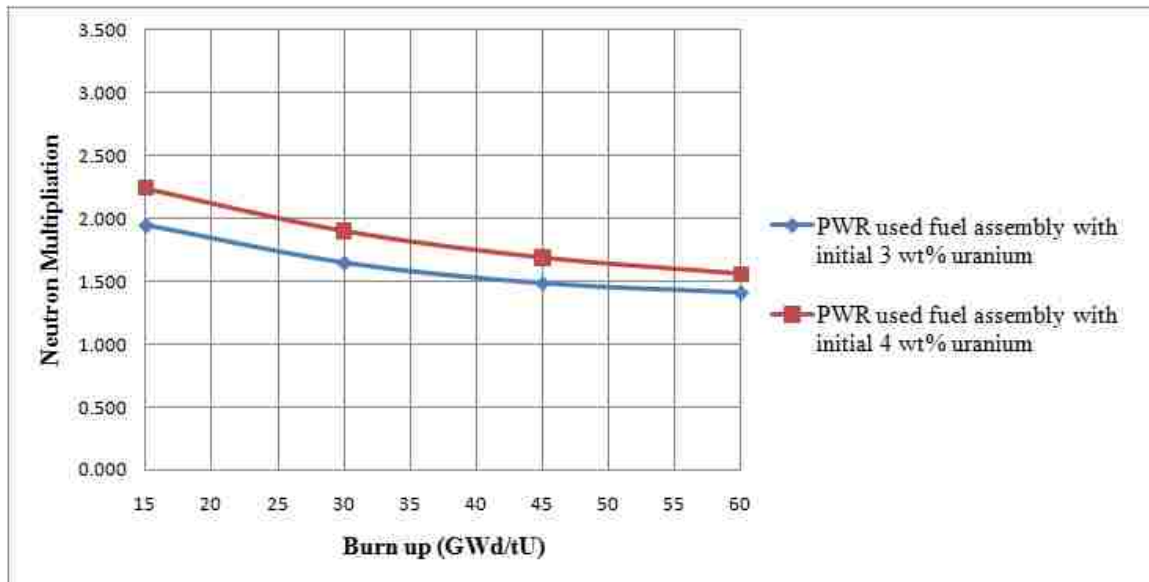


Figure 7. Neutron multiplication with Cd layer for PWR Fuel Assembly 1 and 2.

The cadmium layer was able to prevent more than 10% of thermal neutrons from reflecting back into the fuel increasing the neutron-to-fission reactions with fissile material in used fuel assemblies.

Table VII. MCNPX Data for Neutron Multiplication with Cadmium Layer.

GWd/tU	PWR Fuel Assembly 1	PWR Fuel Assembly 2
15	1.945 ± 0.002	2.244 ± 0.003
30	1.649 ± 0.002	1.903 ± 0.002
45	1.487 ± 0.002	1.689 ± 0.002
60	1.413 ± 0.002	1.559 ± 0.002

The following tables and figures showed the cadmium ratio results as fuel was used for energy production. The results shown are for PWR Fuel Assemblies 1 and 2 with four FC detectors. The Tables VII and VIII included the data used for the figures with propagation errors.

Table VIII. Cadmium Ratio Data for PWR Fuel Assembly 1.

GWd/tU	FC Detector			
	HEU	UO ₂	DU	Thorium
15	1.855 ± 0.009	1.843 ± 0.009	1.800 ± 0.009	1.361 ± 0.013
30	1.677 ± 0.010	1.674 ± 0.010	1.628 ± 0.009	1.243 ± 0.014
45	1.587 ± 0.011	1.587 ± 0.010	1.545 ± 0.010	1.163 ± 0.016
60	1.555 ± 0.011	1.554 ± 0.011	1.505 ± 0.010	1.122 ± 0.015

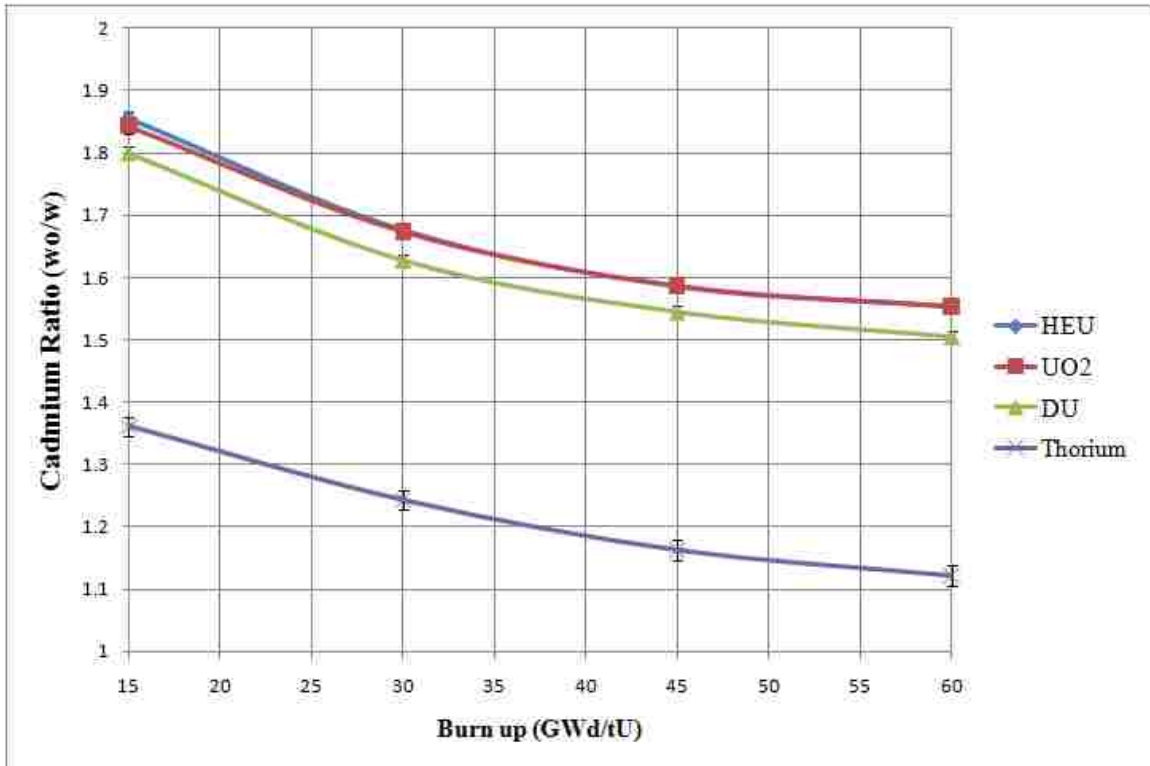


Figure 8. Cadmium Ratio for FC detectors using PWR Fuel Assembly 1.

Comparing the FC detectors cadmium ratio for PWR Fuel Assembly 1, the HEU FC detector has the highest CR; therefore, the PNAR response was higher. The UO₂ FC detector had a similar response to the HEU FC detector, at 15 GWd/tU this was only a 0.6% difference. The DU detector has about 3% lower response to the HEU FC detector.

The greatest difference in response was for thorium FC detectors about 30%, because of thorium insensitivity to thermal neutrons.

Table IX. Cadmium Ratio for PWR Fuel Assembly 2.

GWd/tU	FC Detector			
	HEU	UO ₂	DU	Thorium
15	1.962 ± 0.009	1.968 ± 0.009	1.926 ± 0.009	1.492 ± 0.013
30	1.792 ± 0.010	1.794 ± 0.010	1.748 ± 0.009	1.346 ± 0.014
45	1.665 ± 0.011	1.673 ± 0.010	1.630 ± 0.010	1.230 ± 0.016
60	1.619 ± 0.011	1.635 ± 0.011	1.596 ± 0.010	1.212 ± 0.015

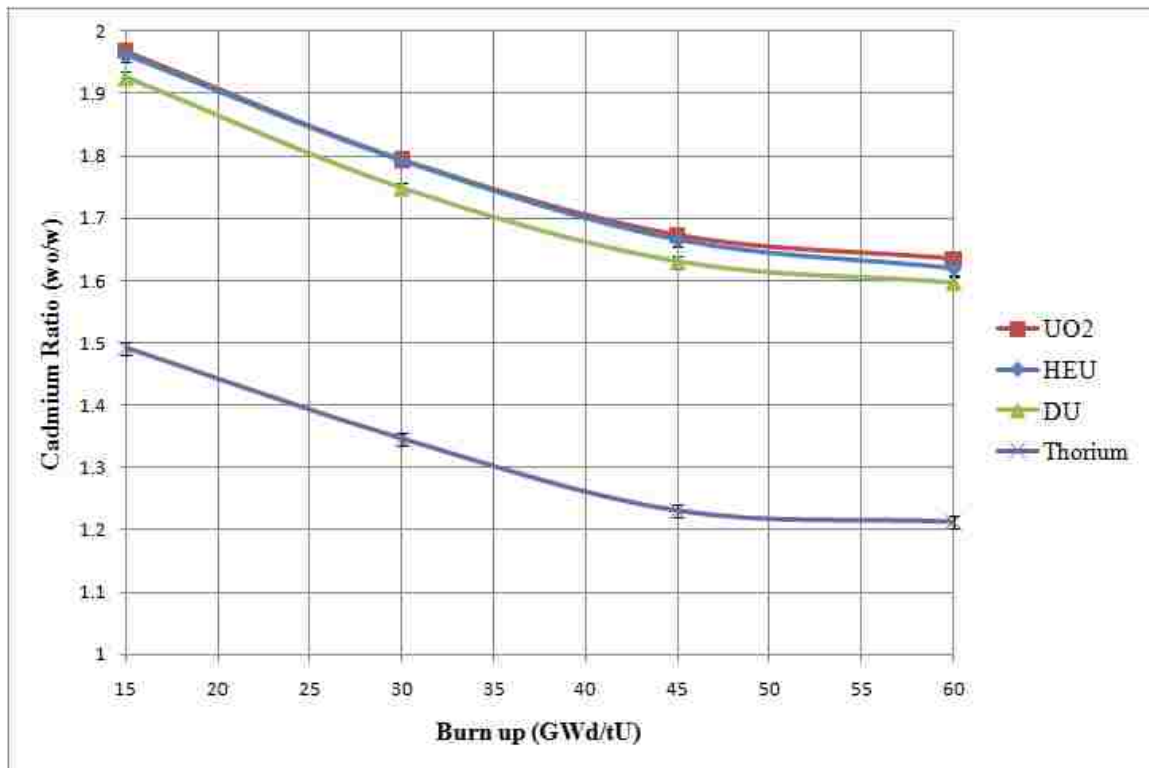


Figure 9. Cadmium ratio for FC detectors using PWR Fuel Assembly 2.

For PWR Fuel Assembly 2, about the same trend in response can be seen. In this case, the UO₂ FC detector had a negligible 0.3% higher response to the HEU FC detector. The DU

detector had about 2% lower response than the HEU FC detector. The thorium FC detector showed the greatest difference in response, about 30%.

Figure 10 compares the most responsive FC detector HEU to the least responsive thorium FC detectors for PWR Fuel Assemblies 1 and 2.

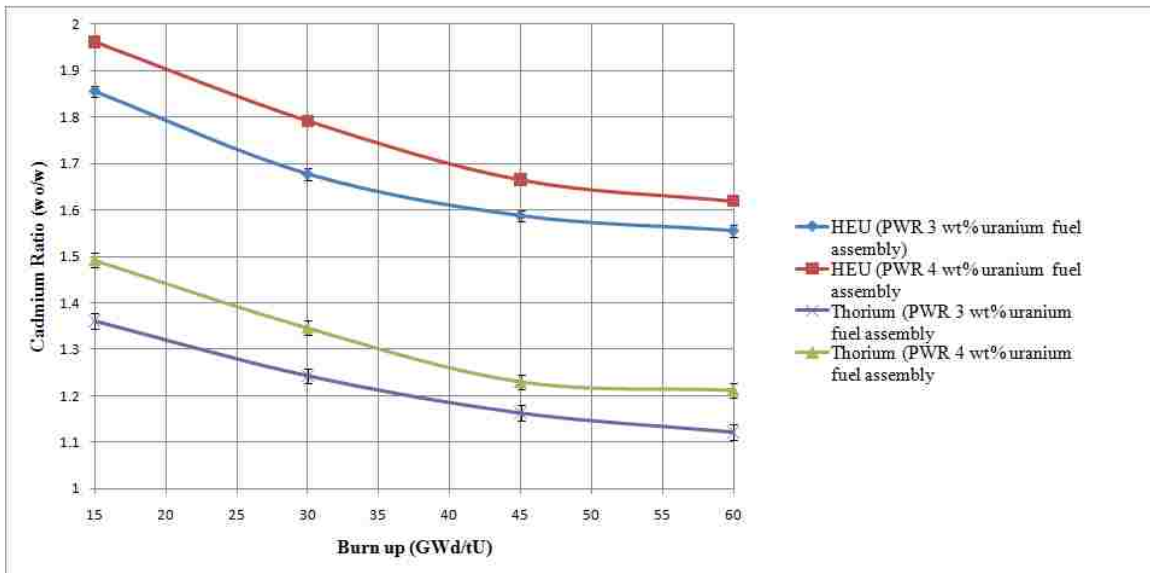


Figure 10. PNAR response using the Cadmium Ratio for HEU and thorium FC.

The response of HEU FC detector for PWR Fuel Assembly 2 was about 5% higher than the HEU FC detector for PWR Fuel Assembly 1. The difference in response was a result of the neutron multiplication being higher for PWR Fuel Assembly 2, due to the additional 1% fissile U-235. The response of the thorium FC detector for PWR Fuel Assembly 2 is about 7.5% higher than for PWR Fuel Assembly 1. Based on the cadmium ratios the HEU FC detector was more responsive for both PWR fuel assemblies 1 and 2. Next, the FC detectors were analyzed using the detector time precision.

Detector Precision and Counting Times

The detector precision was calculated to compare the experimental MCNPX tally results for PWR Fuel Assemblies 1 and 2. The detector time was calculated by setting the relative counting uncertainty to 0.05%. In order to achieve a 0.05% precision, the total counts required are 4×10^6 . The counting times need to be less than 60 seconds, in order to process as many used fuel assemblies as possible. Large counting times will not be useful, because it will be time consuming.

The tables below illustrate the minimum count times, assuming a 100% detector efficiency, for the FC detectors for PWR Fuel Assemblies 1 and 2.

Table X. Minimum Counting Times for FC Detectors using PWR Fuel Assembly 1 at 45 GWd/tU.

FC Detector	Counts per source neutron (MCNPX tally)		Count Rate (neutrons per second)		Counting Time (seconds)	
	with Cd	without Cd	with Cd	without Cd	with Cd	without Cd
HEU	5.95E-04	9.45E-04	2.33E+05	3.70E+05	17 ± 1	11 ± 1
UO ₂	1.11E-04	1.76E-04	4.35E+04	6.90E+04	92 ± 1	58 ± 1
DU	1.31E-06	2.02E-06	5.14E+02	7.92E+02	7789 ± 62	5052 ± 33
Thorium	2.34E-08	2.72E-08	9.17E+00	1.07E+01	436072 ± 4884	375150 ± 4164

The counting times for HEU FC detector for PWR Fuel Assembly 1, was the lowest at about 17 ± 1 seconds. Thorium FC detector had the highest counting time. The difference in acquisitions times was due to higher counts detected in HEU FC detector and a higher count rate. For thorium FC detectors, the neutron counts detected were the lowest and the count rate was the smallest.

Table XI. Minimum Counting Times for FC detectors using PWR Fuel Assembly 2 at 45 GWd/tU.

FC Detector	Counts per source neutron (MCNPX tally)		Count Rate (neutrons per second)		Counting Time (seconds)	
	with Cd	without Cd	with Cd	without Cd	with Cd	without Cd
HEU	6.90E-04	1.15E-03	2.70E+05	4.50E+05	15 ± 1	9 ± 1
UO ₂	1.28E-04	2.15E-04	5.03E+04	8.42E+04	79 ± 1	47 ± 1
DU	1.51E-06	2.47E-06	5.94E+02	9.67E+02	6740 ± 38	4135 ± 30
Thorium	2.64E-08	3.25E-08	1.04E+01	1.27E+01	386163 ± 4164	313934 ± 3601

Table X shows the data for FC detectors using PWR Fuel Assembly 2 and the calculated counting times. For PWR Fuel Assembly 2, the HEU FC detector obtained the smallest acquisition time 15±1 seconds, compared to the other FC detectors. Comparing the counting times for PWR Fuel Assemblies 1 and 2 using the FC detectors, the counting times were about 14% less for PWR Fuel Assembly 1 compared to PWR Fuel Assembly 2. The acquisition times for PWR Fuel Assembly 2 were higher because of the additional fissile U-235, which increased the spontaneous neutron fission count rate.

Fissile Content Measurements

MCNPX results were used to calculate the fissile mass in each of the PWR fuel assemblies modeled. The total fissile isotopes mass for U-235, Pu-239 and Pu-241 were compared to the cadmium ratio. In a used fuel assembly at 15 GWd/tU about 1.5% of the total 533 kilograms belongs to U-235 compared to about 0.4% of Pu-239 mass for PWR Fuel Assembly 1. The accumulated total fissile mass decreases as fuel burn-up increased; however, the mass concentration of Pu-239 and Pu-241 increased. The following figures illustrate the cadmium ratio comparisons with the fissile material and Pu-239 mass concentrations for PWR Fuel Assemblies 1 and 2.

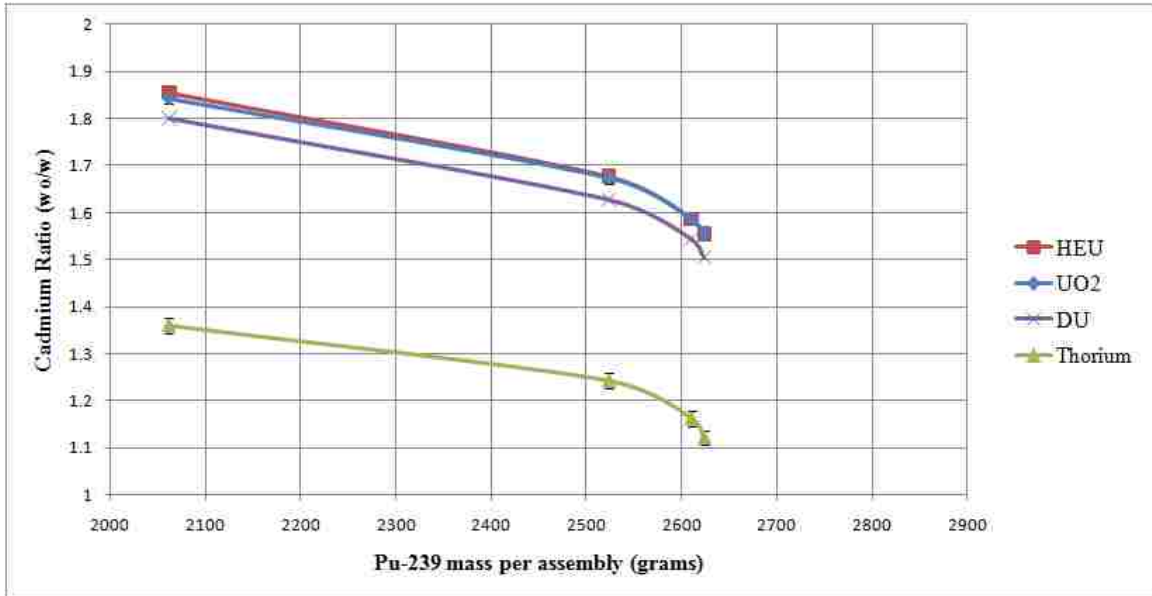


Figure 11. Cadmium Ratio with Pu-239 mass in PWR Fuel Assembly 1.

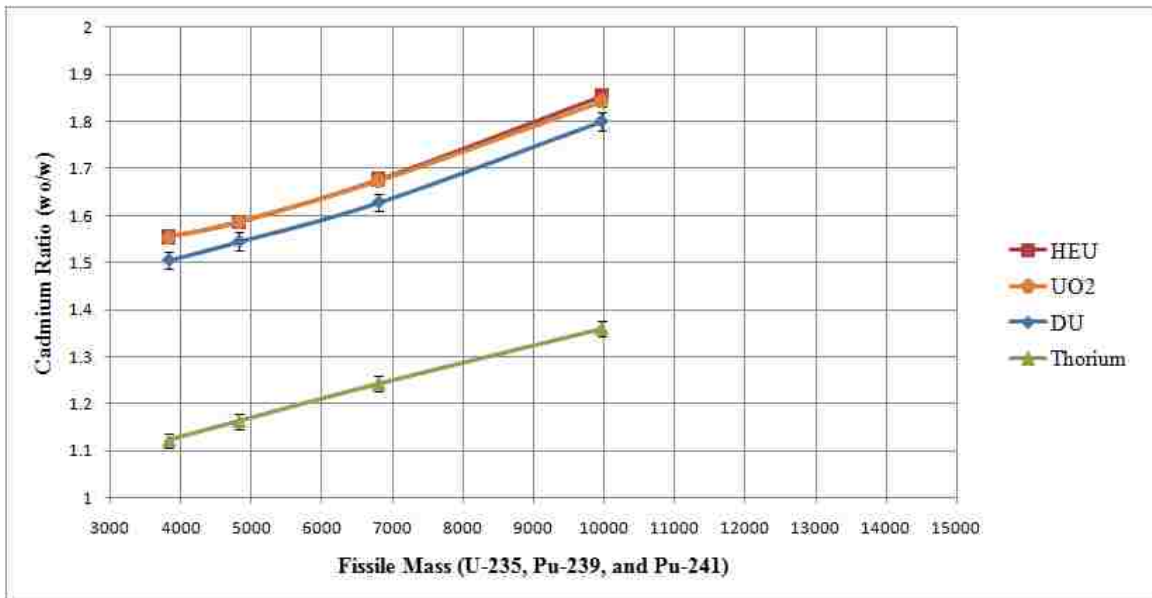


Figure 12. Cadmium Ratio with fissile mass in PWR Fuel Assembly 1.

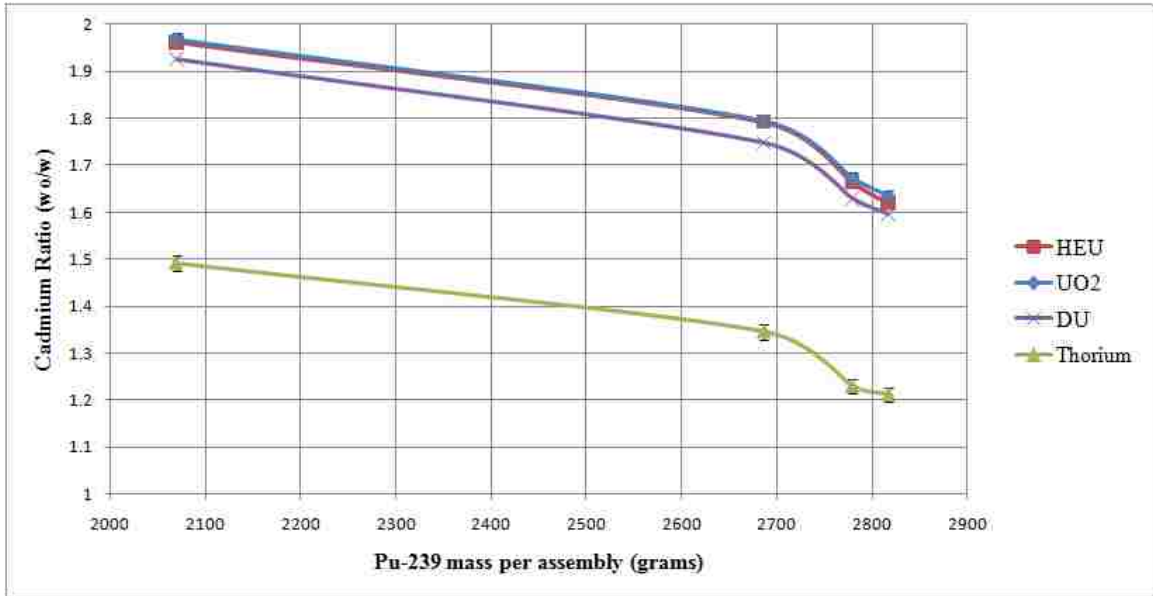


Figure 13. Cadmium Ratio with Pu-239 mass in PWR Fuel Assembly 2.

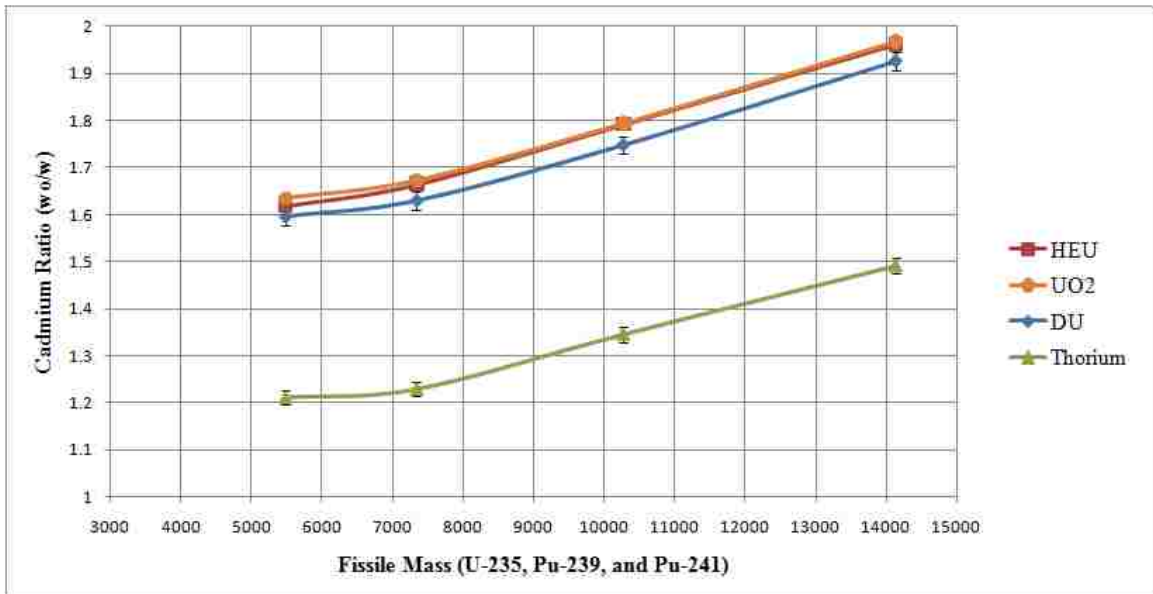


Figure 14. Cadmium Ratio with Fissile mass in PWR Fuel Assembly 2.

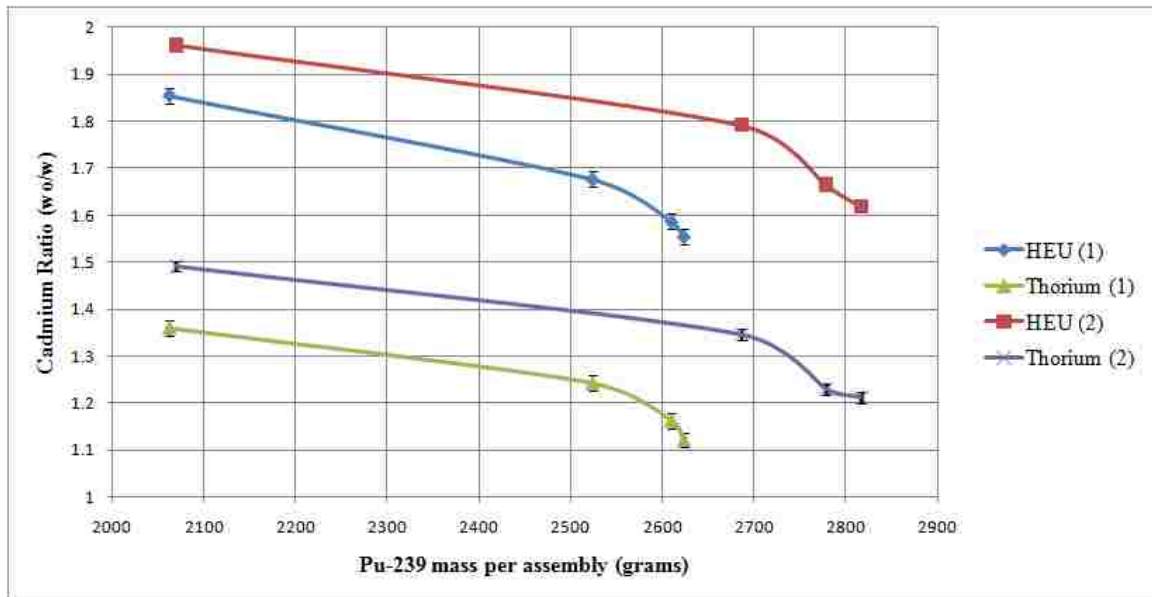


Figure 15. Cadmium Ratio with Pu-239 in for HEU and Thorium FC Detectors.

Comparing the results for HEU and thorium FC detectors, it can be shown the PNAR method responded to change in Pu-239 with different PWR fuel assemblies.

Table XII. Data for Cadmium Ratios with Pu-239 in PWR Fuel Assembly 1.

Pu-239 (grams)	FC Detector	
	HEU (PWR Fuel Assembly 1)	Thorium (PWR Fuel Assembly 1)
2062	1.855 ± 0.009	1.361 ± 0.013
2524	1.677 ± 0.010	1.243 ± 0.014
2610	1.587 ± 0.011	1.163 ± 0.016
2624	1.555 ± 0.011	1.122 ± 0.015

Table XIII. Data for Cadmium Ratios with Pu-239 in PWR Fuel Assembly 2.

Pu-239 (grams)	FC Detector	
	HEU (PWR Fuel Assembly 2)	Thorium (PWR Fuel Assembly 2)
2070	1.962 ± 0.009	1.492 ± 0.013
2686	1.792 ± 0.010	1.346 ± 0.014
2779	1.665 ± 0.011	1.230 ± 0.016
2817	1.619 ± 0.011	1.212 ± 0.015

For PWR Fuel Assembly 1 to PWR Fuel Assemblies 2, the increase in Pu-239 mass and the decrease in cadmium ratio was significantly minor.

The cadmium ratio was compared using HEU and thorium FC detectors. There was about a 30% increase in fissile mass from PWR Fuel Assembly 1 to Fuel Assembly 2; however, only a 5% increase in the cadmium ratio for HEU detectors for PWR Fuel Assemblies 2. The thorium FC detectors showed a 7.5% increase in cadmium ratio. The HEU FC detector still performed 30% better than the thorium FC detectors.

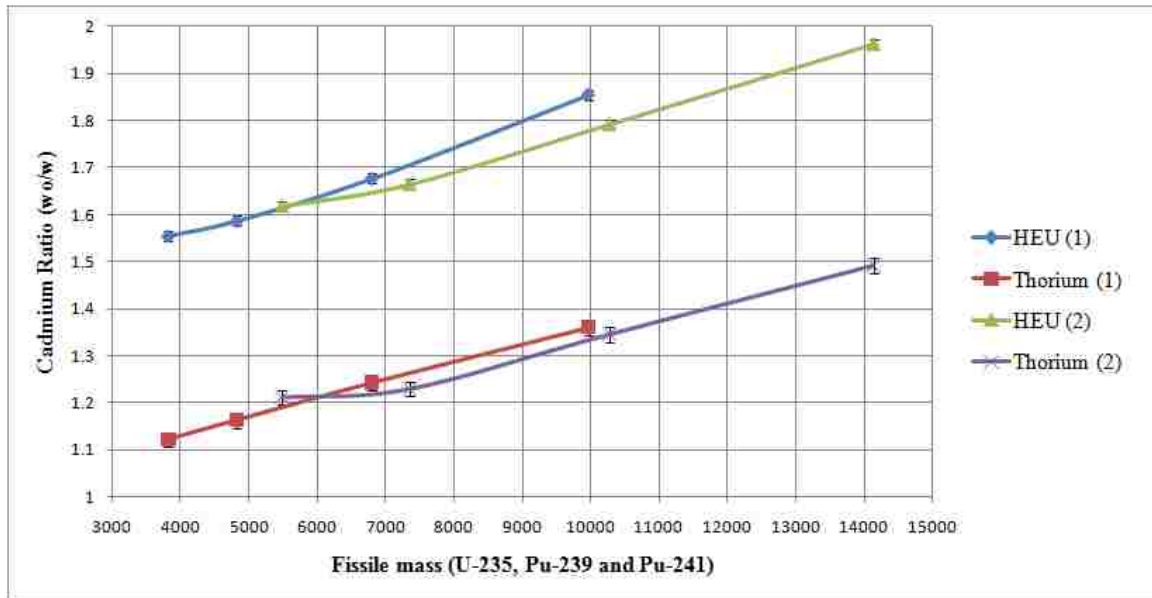


Figure 16. Cadmium Ratio with fissile mass in for HEU and Thorium FC Detectors

Table XIV. Data for Cadmium Ratios with fissile mass in PWR Fuel Assembly 1.

Fissile Mass	FC Detector	
	HEU (PWR Fuel Assembly 1)	Thorium (PWR Fuel Assembly 1)
9970	1.855 ± 0.009	1.361 ± 0.013
6805	1.677 ± 0.010	1.243 ± 0.014
4825	1.587 ± 0.011	1.163 ± 0.016
3826	1.555 ± 0.011	1.122 ± 0.015

Table XV. Data for Cadmium Ratios with fissile mass in PWR Fuel Assembly 2.

Fissile Mass	FC Detector	
	HEU (PWR Fuel Assembly 2)	Thorium (PWR Fuel Assembly 2)
14140	1.962 ± 0.009	1.492 ± 0.013
10275	1.792 ± 0.010	1.346 ± 0.014
7347	1.665 ± 0.011	1.230 ± 0.016
5487	1.619 ± 0.011	1.212 ± 0.015

The PNAR technique responded to the change in fissile mass and Pu-239; however, as an individual technique it does not quantify the plutonium mass or fissile mass in used fuel assemblies.

CHAPTER 5

CONCLUSIONS

MCNPX was used to create simulations using the PNAR technique with four FC detectors and two PWR Fuel Assemblies. The PNAR technique was analyzed using the cadmium ratio and detector counting times to compare the FC detectors. The cadmium ratio scales with fissile material in used fuel assemblies and the counting time was based on the uncertainty of 0.05% for a single measurement. As expected the cadmium ratio decreased with burn up. The analysis demonstrated the HEU FC detector using the PNAR measurement technique performed better and thorium FC detector had the lowest response.

Cadmium ratio analysis using the PNAR measurement technique for both PWR Fuel Assemblies 1 and 2, demonstrated the HEU FC detector performed 0.3% better than UO₂, 3% better than DU and 30% better than thorium FC detectors. HEU FC detectors have a higher sensitivity to thermal neutrons compared to the other FC detectors. Thorium FC detectors lower response demonstrated their tendency to absorb only fast neutrons and their insensitivity to thermal neutrons. The detector counting times showed the HEU FC detector's time was significantly less compared to the other FC detectors.

The PNAR measurement technique was compared to the fissile mass and Pu-239 for PWR Fuel Assemblies 1 and 2 at different energy production rates. The PNAR responded to the change in mass concentrations as energy production rates increased; however, as a single technique it did not assay the elemental plutonium mass in used fuel assemblies. In order to assay plutonium mass more information is needed such as the initial enrichment and burn up of the fuel. Further research is required, a recommendation

in NDA research is to continue using the PNAR with HEU FC detectors and integrate it with another NDA technique to evaluate the capability to quantify plutonium mass in used fuel assemblies.

APPENDIX I MCNPX INPUT

A sample input using MCNPX is provided for a used fuel assembly with initial 3 wt % U-235, cooled for 20 years at a burn rate of 15 GWd/tU using HEU FC detector is displayed. An input deck in MCNPX is created in the three sections cell, surface and data cards. In the cell cards information about the density (grams per cm³) in a surface geometry are found. The surface cards are used to define the geometry. In the data cards information about materials, tallies and physic options are inputted for MCNPX to do its calculation. The materials cards were not included to save space.

C Cell Cards

C Burnup: 15 GWd/tU

C Fuel Pin 1 Dimensions

4	4	-10.4538	-4	16	-17	imp:n=1	u=1	\$ fuel/pellat	
5	5	-10.4538	4	-5	16	-17	imp:n=1	u=1	\$ fuel/pella
6	6	-10.4538	5	-6	16	-17	imp:n=1	u=1	\$ fuel/pella
7	7	-10.4538	6	-10	16	-17	imp:n=1	u=1	\$ fuel/pella
8	100	-5.8736	10	-11	16	-17	imp:n=1	u=1	\$ fuel/clad
9	100	-5.8736	-11	17	-19	imp:n=1	u=1	\$ fuel/clad	
10	100	-5.8736	-11	-16	18	imp:n=1	u=1	\$ fuel/clad	
11	200	-1.00	11:19:-18			imp:n=1	u=1	\$ fuel/water	

C Fuel Pin 2 Dimensions

24	24	-10.4538	-4	16	-17	imp:n=1	u=2	\$ fuel/pell	
25	25	-10.4538	4	-5	16	-17	imp:n=1	u=2	\$ fuel/pel
26	26	-10.4538	5	-6	16	-17	imp:n=1	u=2	\$ fuel/pel
27	27	-10.4538	6	-10	16	-17	imp:n=1	u=2	\$ fuel/pel
28	100	-5.8736	10	-11	16	-17	imp:n=1	u=2	\$ fuel/clad
29	100	-5.8736	-11	17	-19	imp:n=1	u=2	\$ fuel/clad	
30	100	-5.8736	-11	-16	18	imp:n=1	u=2	\$ fuel/clad	
31	200	-1.00	11:19:-18			imp:n=1	u=2	\$ fuel/water	

C Fuel Pin 3 Dimensions

44	44	-10.4538	-4	16	-17	imp:n=1	u=3	\$ fuel/pell	
45	45	-10.4538	4	-5	16	-17	imp:n=1	u=3	\$ fuel/pel
46	46	-10.4538	5	-6	16	-17	imp:n=1	u=3	\$ fuel/pel
47	47	-10.4538	6	-10	16	-17	imp:n=1	u=3	\$ fuel/pel
48	100	-5.8736	10	-11	16	-17	imp:n=1	u=3	\$ fuel/clad
49	100	-5.8736	-11	17	-19	imp:n=1	u=3	\$ fuel/clad	
50	100	-5.8736	-11	-16	18	imp:n=1	u=3	\$ fuel/clad	
51	200	-1.00	11:19:-18			imp:n=1	u=3	\$ fuel/water	

*****NOTE continues to Fuel Pin 39, Fuel pins3-38 are removed to save space*****

C Fuel Pin 39 Dimensions

764 764 -10.4538 -4 16 -17 imp:n=1 u=39 \$ fuel/p
765 765 -10.4538 4 -5 16 -17 imp:n=1 u=39 \$ fuel/
766 766 -10.4538 5 -6 16 -17 imp:n=1 u=39 \$ fuel/
767 767 -10.4538 6 -10 16 -17 imp:n=1 u=39 \$ fuel/
768 100 -5.8736 10 -11 16 -17 imp:n=1 u=39 \$ fuel/cl
769 100 -5.8736 -11 17 -19 imp:n=1 u=39 \$ fuel/cl
770 100 -5.8736 -11 -16 18 imp:n=1 u=39 \$ fuel/cla
771 200 -1.00 11:19:-18 imp:n=1 u=39 \$ fuel/wat

C

C Guide/Instrument Tubes

200 200 -1.00 -30 18 -19 imp:n=1 u=50 \$ Guide/inner water
201 100 -5.8736 30 -31 18 -19 imp:n=1 u=50 \$ Guide/clad
202 200 -1.00 31:-18:19 imp:n=1 u=50 \$ Guide/outer water

C

C Fuel assembly lattice

500 0 -12 13 -14 15 lat=1 imp:n=1 u=70 fill=-8:8 -8:8 0:0
39 38 36 33 30 25 21 14 6 14 21 25 30 33 36 38 39
38 37 35 32 29 24 20 13 5 13 20 24 29 32 35 37 38
36 35 34 31 28 50 19 12 50 12 19 50 28 31 34 35 36
33 32 31 50 27 23 18 11 4 11 18 23 27 50 31 32 33
30 29 28 27 26 22 17 10 3 10 17 22 26 27 28 29 30
25 24 50 23 22 50 16 9 50 9 16 50 22 23 50 24 25
21 20 19 18 17 16 15 8 2 8 15 16 17 18 19 20 21
14 13 12 11 10 9 8 7 1 7 8 9 10 11 12 13 14
6 5 50 4 3 50 2 1 50 1 2 50 3 4 50 5 6
14 13 12 11 10 9 8 7 1 7 8 9 10 11 12 13 14
21 20 19 18 17 16 15 8 2 8 15 16 17 18 19 20 21
25 24 50 23 22 50 16 9 50 9 16 50 22 23 50 24 25
30 29 28 27 26 22 17 10 3 10 17 22 26 27 28 29 30
33 32 31 50 27 23 18 11 4 11 18 23 27 50 31 32 33
36 35 34 31 28 50 19 12 50 12 19 50 28 31 34 35 36
38 37 35 32 29 24 20 13 5 13 20 24 29 32 35 37 38
39 38 36 33 30 25 21 14 6 14 21 25 30 33 36 38 39

501 0 103 -102 -104 105 -101 100 imp:n=1 fill=70

c 502 0 (-103:102:104:-105:101:-100 imp:n=1

c adding the water

3331 20 -1.5 -202 203 205 -204 100 -101

(-103:102:104:-105:101:-100) imp:n=1 \$ layer outside fuel

c ----- Al layer

302 301 -2.7 303 -302 -304 305 315 -316

(202:-203:-205:204:-100:101)

#400 #401 #402 #403 imp:n=1

c 1mm of cd or air

400 303 -8.65 -401 400 205 -204 -316 315 imp:n=1 \$ left
 401 303 -8.65 -202 203 402 -403 -316 315 imp:n=1 \$ top
 402 303 -8.65 -202 203 405 -404 -316 315 imp:n=1 \$ bottom
 403 303 -8.65 -406 407 205 -204 -316 315 imp:n=1 \$ right

c
 =====
 c fission chambers 4
 =====

7711 301 -2.7 -44 -310 309 (45:1310:-1309) imp:n=1 \$ Al
 712 301 -2.7 -47 -308 307 (48:1308:-1307) imp:n=1 \$ Al
 713 301 -2.7 -50 -310 309 (51:1310:-1309) imp:n=1 \$ Al
 714 301 -2.7 -53 -308 307 (54:1308:-1307) imp:n=1 \$ Al

c
 7121 316 -18.95 -45 -1310 1309 (46:2310:-2309) imp:n=1 \$ Uranium
 7122 316 -18.95 -48 -1308 1307 (49:2308:-2307) imp:n=1 \$ Uranium
 7123 316 -18.95 -51 -1310 1309 (52:2310:-2309) imp:n=1 \$ Uranium
 7124 316 -18.95 -54 -1308 1307 (55:2308:-2307) imp:n=1 \$ Uranium

c
 7160 317 -0.00164 -46 -2310 2309 imp:n=1 \$ gas
 7161 317 -0.00164 -49 -2308 2307 imp:n=1 \$ gas
 7162 317 -0.00164 -52 -2310 2309 imp:n=1 \$ gas
 7163 317 -0.00164 -55 -2308 2307 imp:n=1 \$ gas

c
 4410 308 -0.96 -311 (-303:302:304:-305:-100:101)
 (47:308:-307) (50:310:-309) (53:308:-307) (44:310:-309) imp:n=1
 4412 20 -1.5 -312 311 (-303:302:304:-305:-315:316)
 (202:-203:-205:204:-100:101) imp:n=1
 999 0 312 imp:n=0 \$outside world

C Surface Cards

C Fuel Pin

4 cz 0.3900
 5 cz 0.4020
 6 cz 0.4075
 10 cz 0.410
 11 cz 0.475
 12 px 0.63
 13 px -0.63
 14 py 0.63
 15 py -0.63
 16 pz -182.88
 17 pz 182.88 \$ original 365.76 changed to 20cm
 18 pz -182.912
 19 pz 182.91 \$ 365.82 or.

C

C Guide Tube/Instrument Tube

30 cz 0.571

```

31 cz 0.613
C assembly dimensions
C
100 pz -182.94
101 pz 183 $ changed from 366
102 px 10.7099
103 px -10.7099
104 py 10.7099
105 py -10.7099
c adding the 1mm Al for Cd
202 px 11.2
203 px -11.2
204 py 11.2
205 py -11.2
c
c 206 pz -183
222 pz -181
333 pz 181
c Alumium outside layer
302 px 11.32
303 px -11.32
304 py 11.32
305 py -11.32
c TOP Cd layer x-positive
c Right Cd Layer
400 px 11.21
401 px 11.31
c Top Cd Layer
402 py 11.21
403 py 11.31
c bottom Cd layer
404 py -11.21
405 py -11.31
c left
406 px -11.21
407 px -11.31
c placing the U-235 fission chambers
c
c Uranium density =18.95      g/cc
c diameter of FC = 1          inches
c thickness from uranium layer = 3      mg/cm2
c diameter of Uthickness=2.31968
c Distance from Fuel= 1.23
c *****
c      Fission chambers 4
c *****

```

c Aluminum Surface Card
 44 c/x 13.810 0 1.260
 47 c/y 13.810 0 1.260
 50 c/x -13.810 0 1.260
 53 c/y -13.810 0 1.260
 c
 c
 c Uranium outer
 45 c/x 13.810 0 1.160
 48 c/y 13.810 0 1.160
 51 c/x -13.810 0 1.160
 54 c/y -13.810 0 1.160
 c
 c gas inner
 46 c/x 13.810 0 1.15984
 49 c/y 13.810 0 1.15984
 52 c/x -13.810 0 1.15984
 55 c/y -13.810 0 1.15984
 c
 c
 307 py -8.61
 308 py 8.61
 309 px -8.61
 310 px 8.61
 1307 py -8.51
 1308 py 8.51
 1309 px -8.51
 1310 px 8.51
 2307 py -8.5098
 2308 py 8.5098
 2309 px -8.5098
 2310 px 8.5098
 315 pz -30
 316 pz 30
 c water between the fc and last layer of Al
 c ** Polyethylene Sleeve---5cm thick
 311 rpp -16.31 16.31 -16.31 16.31 -30 30
 312 rpp -18.00 18.00 -18.00 18.00 -185 185

c *****
 c Data Cards
 c *****
 c *** Material Cards *****
 c Fuel Cladding Zircaloy
 m100 26054 2.0095E-04
 26056 3.1497E-03

26057 7.2739E-05
 26058 9.6802E-06
 40090 5.1160E-01
 40091 1.1157E-01
 40092 1.7053E-01
 40094 1.7282E-01
 40096 2.7842E-02
 24050 7.6283E-05
 24052 1.4711E-03
 24053 1.6681E-04
 24054 4.1522E-05
 1001 4.4995E-04
 1002 5.1750E-08
 nlib=.70c
 c heavy water
 m222 1002 2
 8016.70c 1
 mt222 hwtr.01t
 c fresh water
 m200 1001 2
 8016 1
 nlib=.70c
 mt200 lwtr.01t
 c Boric Acid Solution (2200 mg B/L)
 m20 5010.70c -4.0450E-04 5011.70c -1.7902E-03
 1001.70c -0.111108 8016.70c -0.886698
 c *****
 c Fission Chamber
 c *****
 c Aluminum metal (2.7 g/cc) (0.0603 atom/b*cm)
 m301 13027.70c 1.0
 c
 c Uranium (fission chamber) (18.95 g/cc) (0.0489 atom/b*cm)
 m316 92235.70c 93.0
 92238.70c 7.0
 c
 c Fission chamber gas (Ar+N2) at 1 atm (0.00164116 g/cc) (0.000025 atom/b*cm)
 m317 11000 0.9600
 7014 0.0400
 c Cadmium (8.65 g/cc) (0.0463 atom/b*cm)
 m303 48106.70c 0.01250 \$ Cadmium
 48108.70c 0.00890
 48110.70c 0.12490
 48111.70c 0.12800
 48112.70c 0.24130
 48113.70c 0.12220

48114.70c 0.28730
 48116.70c 0.07490
 c Poly (CH2) (0.95 g/cc) (0.0408 atom/b*cm)
 m308 1001.70c 2.0
 6000.70c 1.0
 mt308 poly.60t
 m333 7014.70c 0.7851
 8016.70c 0.2149 \$ air rho=-0.00123
 c =====
 FMULT 94236 WIDTH = 1.1 WATT = .2 4 SFYIELD 1
 FMULT 94246 WIDTH = 1.1 WATT = .2 4 SFYIELD 1
 FMULT 96246 WIDTH = 1.1 WATT = .2 4 SFYIELD 1
 FMULT 96248 WIDTH = 1.1 WATT = .2 4 SFYIELD 1
 FMULT 98250 WIDTH = 1.1 WATT = .2 4 SFYIELD 1
 c
 m2235 92235.70c 1
 m2238 92238.70c 1
 m4239 94239.70c 1
 m4241 94241.70c 1
 m4155 64155.70c 1 \$ Gd-155
 m2320 90232.70c 1 \$ Pure Th-232
 c
 c 19% enriched U
 m2352 92235.70c 0.19
 92238.70c 0.81
 8016.70c 2
 c 0.2% depleted U
 m2359 92235.70c 0.002
 92238.70c 0.998
 8016.70c 2
 c material cards for fuel pins
 c Burnup: 15 GWd/tU
 c Pin 1
 m4
 90232 5.160E-10
 91231 1.127E-10
 92233 5.438E-10
 92234 1.377E-06
 92235 5.389E-03
 92236 8.195E-04
 92238 3.194E-01
 93236 1.157E-10
 93237 5.138E-05
 94238 6.325E-06
 94239 1.290E-03
 94240 3.202E-04

94241	6.100E-05	53127	1.146E-05	92236	8.450E-04	46110	1.297E-05
94242	2.551E-05	53129	3.815E-05	92238	3.173E-01	47107	1.502E-10
94244	3.228E-10	54128	2.360E-07	93236	1.172E-10	47109	2.365E-05
95241	9.951E-05	54129	8.349E-10	93237	5.563E-05	48110	4.348E-06
95242	1.106E-08	54130	1.066E-06	94238	7.111E-06	48111	6.123E-06
95243	2.221E-06	54131	1.420E-04	94239	2.139E-03	48112	2.878E-06
96243	2.450E-09	54132	2.656E-04	94240	5.297E-04	48113	6.478E-08
96244	1.616E-07	54134	4.163E-04	94241	1.093E-04	50120	1.132E-06
96245	9.436E-09	54136	6.181E-04	94242	4.751E-05	53127	1.547E-05
96246	3.014E-10	55133	3.336E-04	94244	6.445E-10	53129	4.941E-05
7015	4.192E-08	55134	2.414E-08	95241	1.782E-04	54128	3.094E-07
8016	6.658E-01	55135	8.150E-05	95242	1.930E-08	54129	1.116E-09
8017	1.940E-05	55137	2.052E-04	95243	4.294E-06	54130	1.394E-06
33075	5.511E-08	56138	3.478E-04	96243	4.562E-09	54131	1.723E-04
35079	9.620E-10	59141	2.919E-04	96244	3.088E-07	54132	3.186E-04
35081	9.646E-06	60143	2.512E-04	96245	1.853E-08	54134	4.896E-04
36082	1.925E-07	60145	1.825E-04	96246	6.430E-10	54136	7.394E-04
36083	2.245E-05	60148	9.221E-05	7015	4.362E-08	55133	3.940E-04
36084	4.868E-05	61147	3.457E-07	8016	6.657E-01	55134	2.870E-08
36086	9.331E-05	62147	7.747E-05	8017	1.902E-05	55135	9.332E-05
37085	5.065E-05	62149	1.504E-06	33075	6.594E-08	55137	2.424E-04
37087	1.149E-04	62150	6.217E-05	35079	1.133E-09	56138	4.059E-04
39089	2.105E-04	62151	3.608E-06	35081	1.111E-05	59141	3.373E-04
40090	1.013E-04	62152	2.902E-05	36082	2.298E-07	60143	2.848E-04
40091	2.618E-04	63151	6.036E-07	36083	2.498E-05	60145	2.073E-04
40092	2.751E-04	63152	1.142E-09	36084	5.416E-05	60148	1.084E-04
40093	2.956E-04	63153	2.023E-05	36086	1.014E-04	61147	4.001E-07
40094	3.133E-04	63154	6.273E-07	37085	5.594E-05	62147	8.925E-05
40096	3.122E-04	63155	6.222E-08	37087	1.272E-04	62149	1.850E-06
41093	9.309E-10	64152	3.894E-09	39089	2.302E-04	62150	7.292E-05
42095	3.121E-04	64154	2.610E-06	40090	1.104E-04	62151	4.529E-06
43099	2.991E-04	64155	1.148E-06	40091	2.884E-04	62152	3.635E-05
44101	2.734E-04	64156	6.912E-06	40092	3.047E-04	63151	7.576E-07
46104	2.857E-05	64157	2.908E-08	40093	3.311E-04	63152	1.307E-09
46105	9.601E-05	64158	2.228E-06	40094	3.562E-04	63153	2.540E-05
46106	7.859E-05	64160	1.252E-07	40096	3.546E-04	63154	7.842E-07
46108	2.535E-05	67165	4.757E-09	41093	1.045E-09	63155	8.345E-08
46110	8.045E-06	nlib=.70c		42095	3.551E-04	64152	4.476E-09
47109	1.437E-05	m5		43099	3.480E-04	64154	3.260E-06
48110	2.605E-06	90232	5.311E-10	44101	3.209E-04	64155	1.539E-06
48111	3.860E-06	91231	1.092E-10	46104	3.435E-05	64156	9.621E-06
48112	1.941E-06	92233	5.482E-10	46105	1.308E-04	64157	4.355E-08
48113	4.508E-08	92234	1.500E-06	46106	1.167E-04	64158	3.375E-06
50120	9.065E-07	92235	5.220E-03	46108	4.107E-05	nlib=.70c	

*****Note: the rest of the material cards are not included to save space*****

c source Cm-244

c

sdef cel=d4 rad=fcel=d3 ext=d2 axs=0 0 1 PAR=SF

ds3 s 804 263r 805 263r 806 263r 807 263r

si804 0 0.3899

sp804 -21 1

si805 0.3901 0.4019

sp805 -21 1

si806 0.4021 0.4074

sp806 -21 1

si807 0.4076 0.4099

sp807 -21 1

si2 -30 -20 -10 -0.5 0.5 10 20 30

sp2 0 1 1 0.5 1 0.5 1 1

sb2 0 0.1 0.5 1 5 1 0.5 0.1

si4 L (4<500[-1 0 0]<501) (4<500[0 1 0]<501)

(4<500[0 -1 0]<501) (4<500[1 0 0]<501)

(24<500[-2 0 0]<501) (24<500[0 2 0]<501)

(24<500[0 -2 0]<501) (24<500[2 0 0]<501)

****NOTE: lattice continues for every pin in 17x17 array****

sp4 2.1082E-01 2.1082E-01 2.1082E-01 2.1082E-01 2.1201E-01 2.1201E-01

2.1201E-01 2.1201E-01 2.0945E-01 2.0945E-01 2.0945E-01 2.0945E-01

c *****

c

Tally

c *****

fc24 cell neutrons per cm2s in fission chamber layer

f24:n 7121 7122 7123 7124 T

tf24 5

e24 0e-12 20i 2.5e-9 20i 1e-7 20i 20

c

c Fission reaction rate tally

c

fc34 cell neutrons per cm2s

f34:n 7121 7122 7123 7124 T

sd34 1 1 1 1 1

fm34 (-1 316 -6) \$ 2nd set multiplies by fission cross section of U-235

tf34 5

fq34 f m

e34 0e-12 20i 2.5e-9 20i 1e-7 20i 20

mode n

prdmp j 5e4 j j 5e5

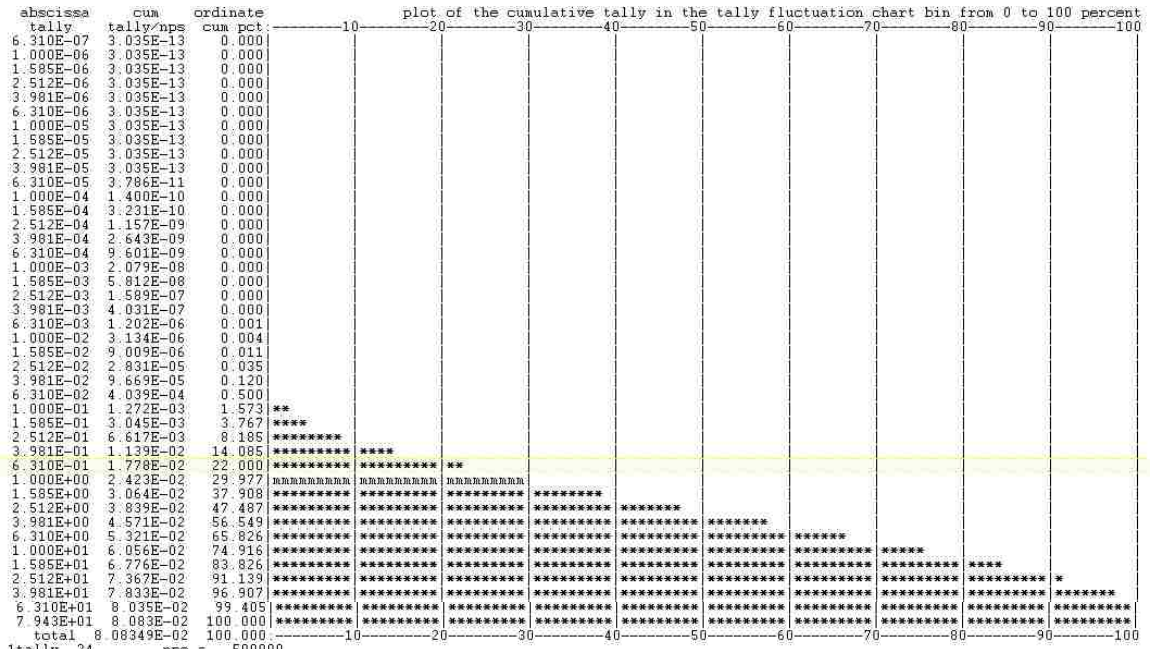
nps 5e+005

print -128

APPENDIX II OUTPUT

A sample output using MCNPX is provided below for a used fuel assembly with initial 3 wt % uranium-235, cooled for 20 years at a burn rate of 15 GWd/tU using HEU FC detector. The first few print screen pages of the output file are a repeat of the input, to save room some part of the input is displayed and not the entire output file is included.

```
lmcnpX version 27b ld=Tue Aug 18 08:00:00 MST 2009 01/16/11 09:28:58
*****
i=C:/sandra/Input/PNAR_FC_3p_15g_1_1_in.o c=C:/sandra/output/PNAR_FC_3p_15g_1_1_in.o r=C:/
warning. universe map (print table 128) disabled.
*****
*
* MCNPX *
*
* Copyright 2007, Los Alamos National Security, LLC. *
* All rights reserved. *
*
* This material was produced under U.S. Government contract *
* DE-AC52-06NA25396 for Los Alamos National Laboratory. *
* which is operated by Los Alamos National Security, LLC *
* for the U.S. Department of Energy. The Government is *
* granted for itself and others acting on its behalf a *
* paid-up, nonexclusive, irrevocable worldwide license in *
* this material to reproduce, prepare derivative works, and *
* works, and perform publicly and display publicly. *
* Beginning five (5) years after June 1, 2006, subject to *
* additional five-year worldwide renewals, the Government *
* is granted for itself and others acting on its behalf *
* a paid-up, nonexclusive, irrevocable worldwide license *
* in this material to reproduce, prepare derivative works, *
* distribute copies to the public, perform publicly and *
* display publicly, and to permit others to do so. *
*
* NEITHER THE UNITED STATES NOR THE UNITED STATES *
* DEPARTMENT OF ENERGY, NOR LOS ALAMOS NATIONAL SECURITY, *
* LLC, NOR ANY OF THEIR EMPLOYEES, MAKES ANY WARRANTY, *
* EXPRESS OR IMPLIED, OR ASSUMES ANY LEGAL LIABILITY OR *
* RESPONSIBILITY FOR THE ACCURACY, COMPLETENESS, OR *
* USEFULNESS OF ANY INFORMATION, APPARATUS, PRODUCT, OR *
* PROCESS DISCLOSED, OR REPRESENTS THAT ITS USE WOULD NOT *
* INFRINGE PRIVATELY OWNED RIGHTS. *
*****
1- IVBA
2- C Cell Cards
3- C Sun Jan 9 23:57:00 2011
```

tally type 4 track length estimate of particle flux units 1/cm**2
 particle(s): neutron

volumes cell: 7121 7122 7123 7124 total
 2.15371E-02 2.15371E-02 2.15371E-02 2.15371E-02 8.61485E-02

cell 7121 energy

0.0000E+00	0.00000E+00	0.0000
1.1905E-10	0.00000E+00	0.0000
2.3810E-10	5.79653E-09	0.6001
3.5714E-10	2.16908E-08	0.5610
4.7619E-10	1.84344E-08	0.5292
5.9524E-10	2.46225E-08	0.3381
7.1429E-10	1.23514E-08	0.4481
8.3333E-10	7.80002E-08	0.4868
9.5238E-10	7.17557E-08	0.5403
1.0714E-09	9.80636E-08	0.4189
1.1905E-09	8.60303E-08	0.5273
1.3095E-09	8.02785E-08	0.3661
1.4286E-09	7.83614E-08	0.2739
1.5476E-09	1.09339E-07	0.3799
1.6667E-09	1.58308E-07	0.3118
1.7857E-09	1.06584E-07	0.5107
1.9048E-09	1.01473E-07	0.2021
2.0238E-09	1.33108E-07	0.2938
2.1429E-09	1.71623E-07	0.2673
2.2619E-09	1.20736E-07	0.4497
2.3810E-09	1.54880E-07	0.3679
2.5000E-09	6.26986E-07	0.8119
7.1429E-09	9.73303E-06	0.0486
1.1786E-08	1.61843E-05	0.0382
1.6429E-08	2.24192E-05	0.0551
2.0000E+01	0.00000E+00	0.0000
total	8.77150E-04	0.0050

analysis of the results in the tally fluctuation chart bin (tfc) for tally 24 with nps = 500000 print table 160

normed average tally per history = 8.77150E-04	unnormed average tally per history = 7.55651E-05
estimated tally relative error = 0.0050	estimated variance of the variance = 0.0024
relative error from zero tallies = 0.0020	relative error from nonzero scores = 0.0046
number of nonzero history tallies = 207407	efficiency for the nonzero tallies = 0.1581
history number of largest tally = 219091	largest unnormalized history tally = 7.03071E-02
(largest tally)/(average tally) = 9.30417E+02	(largest tally)/(avg nonzero tally) = 1.47060E+02
(confidence interval shift)/mean = 0.0001	shifted confidence interval center = 8.77220E-04

if the largest history score sampled so far were to occur on the next history, the tfc bin quantities would change as follows:

estimated quantities	value at nps	value at nps+1	value(nps+1)/value(nps)-1
mean	8.77150E-04	8.78780E-04	0.001859
relative error	5.04100E-03	4.96373E-03	-0.015327
variance of the variance	2.43270E-03	2.95689E-03	0.215478
shifted center	8.77220E-04	8.77357E-04	0.000156
figure of merit	1.12376E+02	1.15901E+02	0.031373

the estimated inverse power slope of the 200 largest tallies starting at 1.20035E-02 is 4.2347
 the large score tail of the empirical history score probability density function appears to have no unsampled regions.

***** the nps-dependent tfc bin check results are suspect because there are only 1 nps tally values to analyze *****

```

ltally 34      nps = 500000      cell neutrons per cm2s
+
tally type 4      track length estimate of particle flux.
particle(s): neutron
multiplier bin 1: -1.00000E+00 316      -6

volumes
cell:      7121      7122      7123      7124      total
1.00000E+00 1.00000E+00 1.00000E+00 1.00000E+00 1.00000E+00

energy bin: 0.      to 0.00000E+00
mult bin: 1
cell
7121      0.00000E+00 0.0000
7122      0.00000E+00 0.0000
7123      0.00000E+00 0.0000
7124      0.00000E+00 0.0000
total     0.00000E+00 0.0000

energy bin: 0.00000E+00 to 1.19048E-10
mult bin: 1
cell
7121      0.00000E+00 0.0000
7122      1.81978E-07 0.8772
7123      2.48097E-08 0.8375
7124      2.89903E-08 1.0000
total     2.35778E-07 0.6937

energy bin: 1.19048E-10 to 2.38095E-10
mult bin: 1
cell
7121      4.52782E-08 0.5985
7122      7.83172E-08 0.5541
7123      2.57461E-08 0.7071
7124      1.23928E-07 0.4985
total     2.73269E-07 0.3010

energy bin: total
mult bin: 1
cell
7121      2.03380E-04 0.0152
7122      1.96094E-04 0.0138
7123      1.98391E-04 0.0152
7124      2.01887E-04 0.0153
total     7.99752E-04 0.0076

lanalysis of the results in the tally fluctuation chart bin (tfc) for tally 34 with nps = 500000      print table 160

normed average tally per history = 7.99752E-04      unnormed average tally per history = 7.99752E-04
estimated tally relative error = 0.0076      estimated variance of the variance = 0.0064
relative error from zero tallies = 0.0020      relative error from nonzero scores = 0.0073

number of nonzero history tallies = 207407      efficiency for the nonzero tallies = 0.1581
history number of largest tally = 146903      largest unnormalized history tally = 1.80768E+00
(largest tally)/(average tally) = 2.26031E+03      (largest tally)/(avg nonzero tally) = 3.57260E+02

(confidence interval shift)/mean = 0.0002      shifted confidence interval center = 7.99910E-04

if the largest history score sampled so far were to occur on the next history, the tfc bin quantities would change as follows:

estimated quantities      value at nps      value at nps+1      value(nps+1)/value(nps)-1.
mean      7.99752E-04      8.03366E-04      0.004519
relative error      7.61237E-03      7.71138E-03      0.013006
variance of the variance      6.42201E-03      8.48441E-03      0.321146
shifted center      7.99910E-04      8.00246E-04      0.000420
figure of merit      4.92793E+01      4.80220E+01      -0.025514

the estimated inverse power slope of the 200 largest tallies starting at 1.98031E-01 is 3.5701
the large score tail of the empirical history score probability density function appears to have no unsampled regions.

***** the nps-dependent tfc bin check results are suspect because there are only 1 nps tally values to analyze *****

```

APPENDIX III CALCULATIONS

1. Atom density of HEU FC detector thin layer

$$\text{Avogadro's Number } (A_{\text{number}}) = 6.02 \times 10^{23} \frac{\text{atoms}}{\text{mole}}$$

$$\rho \text{ (density)} = 18.95 \frac{\text{grams}}{\text{cm}^3}$$

$$\begin{aligned} \text{Mass}_{\text{HEU}} &= \frac{1}{\frac{0.93}{235.0439 \frac{\text{g}}{\text{mole}}} + \frac{0.07}{238.0508 \frac{\text{g}}{\text{mole}}}} \\ &= 235.252 \frac{\text{g}}{\text{mole}} \end{aligned}$$

Therefore;

$$N(\text{atom density}) = \frac{\rho * A_{\text{number}}}{\text{Mass}_{\text{HEU}}}$$

$$N(\text{atom density}) = \frac{18.95 \frac{\text{g}}{\text{cm}^3} * 6.02 \times 10^{23} \frac{\text{atoms}}{\text{mole}}}{235.252 \frac{\text{g}}{\text{mole}}} = 4.851 \times 10^{23} \frac{\text{atoms}}{\text{cm}^3}$$

$$N = 4.851 \times 10^{23} \frac{\text{atoms}}{\text{cm}^3} * 1 \times 10^{-24} \frac{\text{cm}^2}{\text{barn}} \rightarrow N = 4.851 \times 10^{-2} \frac{\text{atoms}}{\text{barn-cm}}$$

2. Tally Multiplier calculations

$$\text{Tally Multiplier} = (\text{Flux tally}) * (\rho_{\text{atom}}) * (\text{Volume}) * (\sigma_{\text{fission}})$$

$$\begin{aligned} &= \left(7.18 \times 10^{-4} \frac{\text{counts}}{\text{cm}^2 \text{ per source neutron}} \right) * (4.851 \times 10^{-2} \frac{\text{atoms}}{\text{barn cm}}) * (2.152 \times 10^{-2} \text{ cm}^3) * (219 \text{ barn}) \\ &= 2.124 \times 10^{-4} \frac{\text{counts}}{\text{source neutron}} \end{aligned}$$

BIBLIOGRAPHY

1. PNNL, P. N. (2008). *AFCI Safeguards Enhancement Study: Technology Development Roadmap*. Richland, WA: PNNL-18099.
2. Evans, L. A. (2010). Nondestructive Determination of Plutonium Mass in Spent Fuel: Preliminary Modeling Results using the Passive Neutron Albedo Reactivity Technique. *Publication in Proceedings of Waste Management 2010*. Phoenix, AZ: LANL.
3. Fensin, M. T. (2009). *A Monte Carlo Based Spent Fuel Analysis Safeguards Strategy Assessment*. Los Alamos: LANL.
4. Conlin, J. (2010). *Determining Fissile Content in PWR Spent Fuel Assemblies Using a Passive Neutron Albedo Reactivity with Fission Chambers Technique*. Los Alamos, NM: LA-UR-10-03566.
5. Swinhoe, M. T. and Tobin, S. J. (2008). An Integrate Approach for Determining Plutonium Mass in Spent Fuel Assemblies with Nondestructive Assay. Los Alamos, NM: LA-UR 08-07888.
6. Tobin, S.J. (2008). *Determining Plutonium in Spent fuel with Nondestructive Assay Techniques*. Los Alamos: LANL.
7. Marietta, M. (1988). *Assessment of Shielding Analysis Methods, Codes, and Data for Spent Fuel Transport/Storage Applications*. Oak Ridge National Laboratory (ORNL).
8. Lamarsh, J. R. (2001). *Introduction to Nuclear Engineering, 3rd edition*. New Jersey: Prentice Hall, Inc.
9. Knoll, G. F. (2000). *Radiation Detection and Measurement, 3rd Ed*. John Wiley & Sons, Inc. 505.
10. Shea, D. A. (2010). The Helium-3 Shortage: Supply, Demand, and Options for Congress. Congressional Research Service.
11. Prasad, K. (1996). Uranium-233 fission detectors for neutron flux measurement in reactors. *Rev. Sci. Instrum.* , 2197.
12. Mohindra, V. (2007). Fission chambers for CANDU SDS neutronic trip applications. *28th Annual Canadian Nuclear Society Conference* (p. 1). Saint John, New Brunswick: CNS.
13. Ensslin, N.K. (1991). The Origin of Neutron Radiation. In D. Reilly, *Passive Nondestructive Assay of Nuclear Material (PANDA)* (p. 339). Los Alamos, NM: LANL.
14. Ensslin, N. K. (1991). Passive Neutron Multiplicity Counting. In D. Reilly, *Passive Nondestructive Assay of Nuclear Material (PANDA)* (pp. 6-1). Los Alamos, NM: LANL.

15. MCNPX Team. (2007). *MCNPX User's Manual, Version 2.6d*. Los Alamos, NM: LA-UR-07-4137, LANL.
16. LaFleur, A. C. (2008). *Nondestructive Measurements of Fissile Material Using Self-Indication Neutron Resonance Absorption Densitometry (SINRA)*. Los Alamos, NM: LA-UR-08-1804, LANL.
17. Phillips, J. (1991). Irradiated Fuel Measurements. In D. Reilly, *Passive Nondestructive Assay of Nuclear Material - PANDA* (p. 551). Los Alamos, NM: LANL.
18. Chart of Nuclides and Isotopes. (2002). *Chart of Nuclides and Isotopes 16th edition*. Lockheed Martin.
19. Fensin, M. T. (2009). Determining Plutonium Mass in Spent Fuel with Nondestructive Assay Techniques- Preliminary Modeling Results Emphasizing Integration among Techniques. *Proceedings of Global 2009*. Paris, France: LBNL.
20. L.P.KU, H. H. (1989). Calculation of the absolute detection efficiency of a moderated ²³⁵U neutron detector on the Tokamak Fusion Test Reactor. *Nuclear Instruments and Methods in Physics Research A* , 113-122.
21. Menlove, N. M. (1994). *The Use of Curium Neutrons to Verify Plutonium in Spent Fuel and Reprocessing Wastes*. Los Alamos: LANL.
22. Parks, C. B. (1988). *Assessment of Shielding Analysis Methods, Codes, and Data for Spent Fuel Transport/Storage Applications*. Oak Ridge, TN: Oak Ridge National Laboratory (ORNL).
23. Rael, C. M. (2004). Neutron Energy Measurements for Impure Plutonium Samples. *45th Annual INMM Meeting*. Orlando, FL: LA-UR-04-0450.
24. Stevens, R. (2008). *Material Control and Accounting (overview)*.
25. Stewart, J. Principles of Total Neutron Counting. In *PANDA*. Los Alamos National Laboratory.

VITA

Graduate College
University of Nevada, Las Vegas

Sandra De La Cruz

Degrees:

Bachelor of Science, Mechanical Engineering, 2008
University of Nevada, Las Vegas

Thesis Title:

Computational Study of Passive Neutron Albedo Reactivity (PNAR) Measurement with
Fission Chambers

Thesis Examination Committee:

Chairperson, Dr. William Culbreth, Ph.D.
Committee member, Dr. Denis Beller, Ph.D.
Committee member, Dr. Robert Boehm, Ph.D.
Graduate Faculty Representative, Dr. Gary Cerefice, Ph.D.